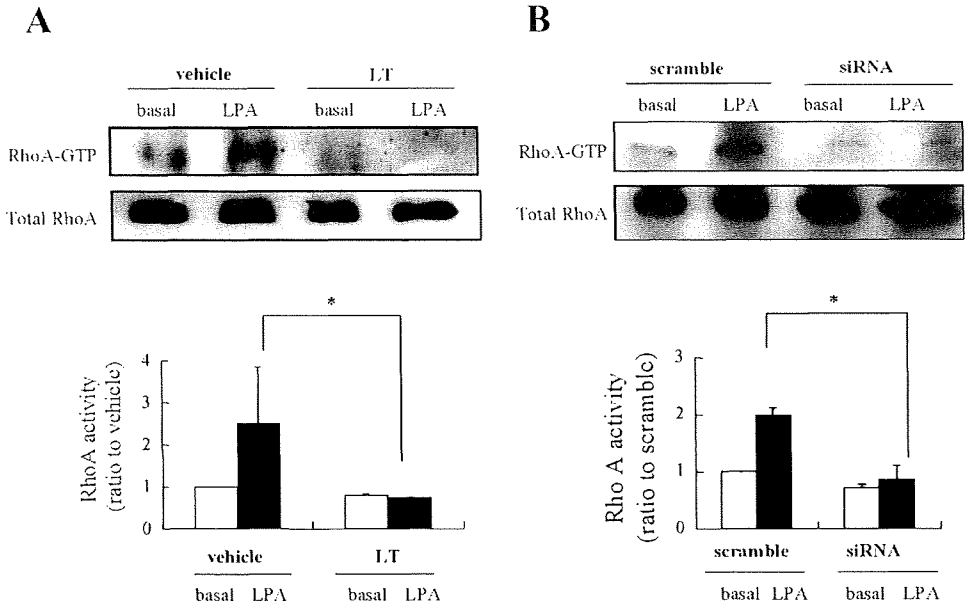

Fig. 7. Effect of PILSAP inhibition or knockdown on RhoA activation upon LPA stimulation. A: Parental MSS31 cells were incubated on type-I collagen for 10 h in 1% FBS/αMEM with or without LT (10 μmol/L). Next, cells were treated with or without LPA (10 μmol/L) for 5 min, and RhoA activity was determined. The values are expressed as the mean ± SD from three independent experiments; *P < 0.05. B: Parental MSS31 cells were transfected with PILSAP siRNA and cells were incubated in 1%FBS/αMEM for 24 h. Then, transfected cells were plated onto type-I collagen coated dishes and incubated for 10 h. Next, cells were treated with or without LPA (10 μmol/L) for 5 min, and RhoA activity was determined. GTP-RhoA was quantified by the density and normalized to that of total RhoA. The values are expressed as the mean ± SD from two independent experiments; *P < 0.05.

activation is not specific during cell adhesion but rather a general component.

Discussion

The present study reveals for the first time that PILSAP takes part in the regulation of RhoA activation in ECs. We have previously reported that PILSAP is involved in S6K activation by catalyzing its upstream partner PDK1 (Yamazaki et al., 2004). Thus, RhoA is noted as another target of PILSAP among the intracellular signaling pathways.

Amid three representative Rho family small GTPases, Rac and cdc42 stimulate protrusion formation at the leading edge and cause membrane ruffle formation, a remodeling of cortical actin (Lauffenburger and Horwitz, 1996; Doughman et al., 2003), whereas RhoA stimulates F-actin formation for contraction of the cell body and the trailing edge. Cdc42 regulates cell migration direction (Raftopoulou and Hall, 2004). The phenotype of Mut-PILSAP transfectants with defective activation of RhoA was quite logical, as they showed aborted F-actin formation and cell polarity.

The importance of RhoA for EC organization during angiogenesis has been documented by Hoang et al. (2004). In that report, constitutive active RhoA stimulated ECs to form vessels with functional lumens while dominant negative RhoA impaired assembly of ECs for neovessel formation. Consistent with that report, network formation by mouse endothelial MSS31 cells on Matrigel was prevented by Mut-PILSAP transfection as well as in the presence of Rho kinase inhibitor (Y27632).

Rho family small GTPases are activated by various extracellular signals through transmembrane proteins including integrins and GPCRs (Karnoub et al., 2004). Among various integrins, β1 integrins support the activation of RhoA, which is associated with a random mode of cell migration (Danen et al., 2005).

GPCRs exhibit a common structural motif consisting of seven membrane-spanning regions (Dohlman et al., 1987), and can be activated by a diverse array of external stimuli, including vasoactive polypeptides, chemoattractants, neurotransmitters, hormones, phospholipids, odorants, and taste ligands (Fukuhara et al., 2001). In general, agonists provoke rapid conformational changes in transmembrane α helices, resulting in exposure of previously masked G protein binding sites in intracellular loops (Altenbach et al., 1996; Bourne, 1997; Wess, 1997). This causes the exchange of GDP for GTP bound to G protein α-subunits or βγ-complexes, and then the initiation of the intracellular signaling response by acting on a variety of effecters. In our study, PILSAP-dependent RhoA activation in ECs is shown not only during cell adhesion but also upon stimulation of PARs or LPA receptor. Thus, PILSAP is rather a general player for RhoA activation in ECs.

Rho family small GTPases act as molecular switches by cycling between GTP- and GDP-bound states. The GTP/GDP cycle is tightly regulated by 3 distinct families of proteins; guanine nucleotide exchange factors (GEFs), GTPase-activating proteins (GAPs) and the guanine nucleotide dissociation inhibitors (GDIs) (Symons and Settleman, 2000). Among them, GEFs activate GTPases by catalyzing the exchange of GDP for GTP, thereby increasing the levels of GTP-bound forms (Donovan et al., 2002; Schmidt and Hall, 2002). More than 70 GEFs have been isolated for Rho family small GTPases (RhoGEFs; Rossman et al., 2005). Whereas many RhoGEFs are highly promiscuous and activate plural Rho family small GTPases, some show activity restricted to a single GTPase (Karnoub et al., 2004). p115-RhoGEF is regarded as a prototype of such RhoA specific GEFs (Hart et al., 1996; Holinstat et al., 2003). Since the requirement of PILSAP was selective to RhoA activation, we employed p115-RhoGEF as a model in our system. Whereas expression of p115-RhoGEF of the mRNA and protein levels were equivalent among Mock, Wt-PILSAP

and Mut-PILSAP transfectants, the GDP/GTP exchanging activity of p115-RhoGEF was significantly lower in Mut-PILSAP transfectants (data not shown).

PARs constitute a subclass of GPCRs that convert extracellular serine protease activity to intracellular signaling events. Proteolysis of PARs results in the cleavage of specific sites in the extracellular domain and formation of a new N-terminus that functions as a tethered ligand. Four types (PAR1, PAR2, PAR3, and PAR4) of this receptor class have been identified in mammals. PAR1, 3 and 4 are activated essentially by thrombin, whereas PAR2 can be activated by trypsin (Cottrell et al., 2002). ECs express at least PAR1 and PAR2 (Brass and Molino, 1997). RhoA-GTP was robustly activated by PAR1 stimulation, but only weakly by PAR2 stimulation by receptor-selective concentration of agonist peptides, and activity of RhoA-GTP and myosin light chain phosphorylation is required for PAR1-mediated monolayer permeability (Klarenbach et al., 2003). Moreover, recent studies have revealed that PARs are involved in vascular development and other biological processes including vascular remodeling (Barnes et al., 2004). The LPA receptor belongs to the endothelial differentiation gene (EDG), also known as the sphingosine 1-phosphate (S1P) receptor family of GPCRs. S1P has the potential to act through endothelial EDG1, EDG3 and probably EDG5, whereas LPA is limited to EDG2 and/or EDG4 (Panetti, 2002). LPA and S1P are important regulators of the vascular system, including angiogenesis and vascular permeability (Panetti, 2002). Thus, the involvement of PILSAP in downstream signaling of PARs and LPA receptor indicate that PILSAP should function in the broad range of vascular pathophysiology.

In summary, the present study reveals for the first time that PILSAP takes part in the regulation of RhoA activation in ECs. This data should provide clues to devise a novel strategy for the regulation of EC function during various processes including angiogenesis.

Acknowledgments

This work was supported by grant-in-aid for Scientific Research on Priority Areas of the Japanese Ministry of Education, Science, Sports and Culture from the Ministry of Education, Science, Sports and Culture of Japan (16022205 and 17014006).

Literature Cited

Akada T, Yamazaki T, Miyashita H, Niizeki O, Abe M, Sato A, Satomi S, Sato Y. 2002. Puromycin insensitive leucyl-specific aminopeptidase (PILSAP) is involved in the activation of endothelial integrins. J Cell Physiol 193:253–262.

Alblas J, Ulfman L, Hordijk P, Koenderman L. 2001. Activation of RhoA and ROCK are essential for detachment of migrating leukocytes. Mol Biol Cell 12:2137–2145.

Altenbach C, Yang K, Farrens DL, Farahbakhsh ZT, Khorana HG, Hubbell WL. 1996. Structural features and light-dependent changes in the cytoplasmic interhelical E-F loop region of rhodopsin: A site-directed spin-labeling study. Biochemistry 35:12470–12478.

Barnes JA, Singh S, Gomes AV. 2004. Protease activated receptors in cardiovascular function and disease. Mol Cell Biochem 263:227–239.

Bourne HR. 1997. How receptors talk to trimeric G proteins. Curr Opin Cell Biol 9:134–142.

Brass LF, Molino M. 1997. Protease-activated G protein-coupled receptors on human platelets and endothelial cells. Thromb Haemost 78:234–241.

Brooks PC, Clark RA, Cheresh DA. 1994. Requirement of vascular integrin αvβ3 for angiogenesis. Science 264:569–571.

Collo G, Pepper MS. 1999. Endothelium cell integrin α5β1 expression is modulated by cytokines and during migration in vitro. J Biol Chem 270:26931–26939.

Cottrell GS, Coelho AM, Bunnett NW. 2002. Protease-activated receptors: The role of cell-surface proteolysis in signaling. Essays Biochem 38:169–183.

Danen EH, van Rheenen J, Franken W, Huveneers S, Sonneveld P, Jalink K, Sonnenberg A. 2005. Integrins control motile strategy through a Rho-cofilin pathway. J Cell Biol 169:515–526.

Dohlman HG, Caron MG, Lefkowits RJ. 1987. A family of receptors coupled to guanine nucleotide regulatory proteins. Biochemistry 26:2657–2664.

Donovan S, Shannon KM, Bollag G. 2002. GTPase activation proteins: Critical regulators of intracellular signaling. Biochem Biophys Acta 1602:23–45.

Doughman RL, Firestone AJ, Wojtasiak ML, Bunce MW, Anderson RA. 2003. Membrane ruffling requires coordination between type I alpha phosphatidylinositol phosphate kinase and Rac signaling. J Biol Chem 278:23036–23045.

Fukuhara S, Chikumi H, Gutkind JS. 2001. RGS-containing RhoGEFs: The missing link between transforming G proteins and Rho? Oncogene 20:1661–1668.

Hart MJ, Sharma S, elMasry N, Qiu RG, McCabe P, Polakis P, Bollag G. 1996. Identification of a novel guanine nucleotide exchanging factor for the Rho GTPase. J Biol Chem 271:25452–25458.

Hoang MV, Whelan MC, Senger DR. 2004. Rho activity critically and selectively regulates endothelial cell organization during angiogenesis. Proc Natl Acad Sci USA 17:1874–1879.

Holinstat M, Mehta D, Kozasa T, Minshall RD, Malik AB. 2003. Protein kinase Cα-induced p115 RhoGEF phosphorylation signals endothelial cytoskeletal rearrangement. J Biol Chem 278:28793–28798.

Hooper NM. 1994. Families of zinc metalloproteases. FEBS Lett 354:1–6.

Iwasaka C, Tanaka K, Abe M, Sato Y. 1996. Ets-1 regulates angiogenesis by inducing the expression of urokinase-type plasminogen activator and matrix metalloproteinase-1 and the migration of vascular endothelial cells. J Cell Physiol 169:522–531.

Karnoub AE, Symous M, Campbell SL, Der CJ. 2004. Molecular basis for Rho GTPase signaling specificity. Breast Cancer Res Theat 84:61–71.

Klarenbach SW, Chipiuk A, Nelson RC, Hollenberg MD, Murray AG. 2003. Differential actions of PAR2 and PAR1 in stimulating human endothelial cell exocytosis and permeability: The role of Rho-GTPases. Circ Res 92:272–278.

Lauffenburger DA, Horwitz AF. 1996. Cell migration: A physically integrated molecular process. Cell 84:359–369.

Li S, Huang NF, Hsu S. 2005. Mechanotransduction in endothelial cell migration. J Cell Biochem 96:1110–1126.

Minambres R, Guasch RM, Perez-Arago A, Guerri C. 2006. The RhoA/ROCK-I/MLC pathway is involved in the ethanol-induced apoptosis by anoikis in astrocytes. J Cell Sci 119:271–282.

Miyashita H, Yamazaki T, Akada T, Niizeki O, Ogawa M, Nishikawa S, Sato Y. 2002. A mouse orthologue of puromycin-insensitive leucyl-specific aminopeptidase is expressed in endothelial cells and plays an important role in angiogenesis. Blood 99:3241–3249.

Niizeki O, Miyashita H, Yamasaki T, Akada T, Abe M, Yoshida N, Watanabe T, Yoshimatsu H, Sato Y. 2004. Transcriptional regulation of angiogenesis-related puromycin-insensitive leucyl-specific aminopeptidase in endothelial cells. Arch Biochem Biophys 424:63–71.

Nobes CD, Hall A. 1999. Rho GTPase control polarity, protrusion, and adhesion during cell movement. J Cell Biol 144:1235–1244.

Oda N, Abe M, Sato Y. 1999. ETS-1 converts endothelial cells to the angiogenic phenotype by inducing the expression of matrix metalloproteinases and integrin β3. J Cell Physiol 178:121–132.

Panetti TS. 2002. Differential effects of sphingosine 1-phosphate and lysophosphatidic acid on endothelial cells. Biochem Biophys Acta 1582:190–196.

Raftopoulou M, Hall A. 2004. Cell migration: Rho GTPases lead the way. Dev Biol 265:23–32.

Rossman KL, Der CJ, Sondek J. 2005. GEF means go: Turning of RHO GTPase with guanine nucleotide-exchanging factors. Nat Rev Mol Cell Biol 6:167–180.

Schmidt A, Hall A. 2002. Guanine nucleotide exchange factors for Rho GTPases: Turning on the switch. Gene Dev 16:1587–1609.

Serwold T, Gonzalez F, Kim J, Jacob R, Shastri N. 2002. ERAAP customizes peptides for MHC class I molecules in the endoplasmic reticulum. Nature 419:480–483.

Sheetz MP, Felsenfeld DP, Galbraith CG. 1998. Cell migration: Regulation of force on extracellular-matrix-integrin complexes. Trends Cell Biol 8:51–54.

Shibuya T, Watanabe K, Yamashita H, Shimizu K, Miyashita H, Abe M, Moriya T, Ohta H, Sonoda H, Shimosegawa T, Tabayashi K, Sato Y. 2006. Isolation and characterization of vasohibin-2 as a homologue of VEGF-inducible endothelium-derived angiogenesis inhibitor vasohibin. Arterioscler Thromb Vasc Biol 26:1051–1057.

Small JV, Stradal T, Vignal E, Rottner K. 2002. The lamellipodium: Where motility begins. Trends Cell Biol 12:112–120.

Symons M, Settleman J. 2000. Rho family GTPases: More than simple switches. Trends Cell Biol 10:415–419.

Taylor A. 1993. Aminopeptidases: Structure and function. FASEB J 7:290–298.

Vouret-Craviari V, Grall D, Van Obberghen-Schilling E. 2003. Modulation of Rho GTPase activity in endothelial cells by selective proteinase-activated receptor (PAR) agonists. J Thromb Haemost 5:1103–1111.

Wess J. 1997. G-protein-coupled receptors: Molecular mechanisms involved in receptor activation and selectivity of G-protein recognition. FASEB J 11:346–354.

Yamazaki T, Akada T, Niizeki O, Suzuki T, Miyashita H, Sato Y. 2004. Puromycin-insensitive leucyl-specific aminopeptidase (PILSAP) binds and catalyzes PDK1, allowing VEGF-stimulated activation of S6K for endothelial cell proliferation and angiogenesis. Blood 104:2345–2352.

Yanai N, Satoh T, Obinata M. 1991. Endothelial cells create a hematopoietic inductive microenvironment preferential to erythropoiesis in the mouse spleen. Cell Struct Funct 16:87–93.

The Vasohibin Family

A Negative Regulatory System of Angiogenesis Genetically Programmed in Endothelial Cells

Yasufumi Sato, Hikaru Sonoda

Abstract—Biological phenomena are under the precise control by the genome. For the regulation of angiogenesis, proangiogenic genes such as VEGFs and angiopoietins are highly conserved, act specifically on endothelial cells, and play a fundamental role. In this sense, nature should prepare specific antiangiogenic genes as well. However, this counterpart of genomic regulation of angiogenesis remains to be established. We recently isolated a novel endothelium-derived angiogenesis inhibitor and named it vasohibin. Vasohibin is dominantly expressed in endothelial cells, induced by the stimulation with VEGF or FGF-2, and selectively affects on endothelial cells and inhibits angiogenesis. Although the mechanism of how vasohibin inhibits angiogenesis remains to be elucidated, our discovery of vasohibin as an endothelium-derived VEGF-inducible angiogenesis inhibitor should shed light on the genomic basis of the negative regulation of angiogenesis. (***Arterioscler Thromb Vasc Biol.* 2007;27:37-41.**)

Key Words: endothelial cell ■ angiogenesis inhibitor ■ VEGF ■ negative feedback

Blood vessels are one of the most quiescent tissues in the body, but have the capacity to form neovessels under certain conditions. Angiogenesis, ie, the formation of neovessels from existing ones, is a key event in various processes that takes place under physiological and pathologic conditions. Physiological conditions include embryonic development, reproduction, and wound healing; whereas pathologic conditions include cancers, proliferative retinopathy, and rheumatoid arthritis. Angiogenesis consist of multiple sequential steps: detachment of mural pericytes for vascular destabilization, extracellular matrix degradation by endothelial proteases, migration of ECs, proliferation of ECs, tube formation by ECs, and reattachment of pericytes for vascular stabilization.[1]

The local balance between angiogenesis stimulators and inhibitors regulates angiogenesis. Understanding of the mechanism of angiogenesis regulation has advanced significantly since the discovery of endothelium-specific proangiogenic factors, namely vascular endothelial growth factor (VEGF) and angiopoietins (Ang) family proteins. VEGFs bind to specific VEGF receptors (VEGFRs), while Angs bind to a tyrosine kinase receptor having Ig and EGF homology domains (TIE) receptor expressed exclusively in the endothelium. Among the VEGF family members, VEGF-A is the most important factor for angiogenesis, stimulating protease synthesis, migration, and proliferation of endothelial cells (ECs), and most of the VEGF-A–mediated signals are transduced via VEGFR-2.[2] TIE-2–mediated signals determine vascular maturation by the pericyte attachment. Amid Ang family members (Ang 1–4), Ang-1 and Ang-3/4 are agonistic ligands, whereas Ang-2 is a very weak ligand and acts as an antagonist of TIE-2 receptor.[3] Ang3 (mouse) and Ang4 (human) are interspecies orthologs.[4]

Various molecules are listed as angiogenesis inhibitors.[5] Most of them, such as pigment epithelium derived factor (PEDF), platelet factor 4, angiostatin, and endostatin, are extrinsic to ECs. In addition, ECs themselves have the capacity to express some angiogenesis inhibitors, eg, soluble VEGFR-1 (sVEGFR-1), vascular endothelial growth inhibitor (VEGI), Down syndrome critical region gene 1 (DSCR1), and vasohibin.

The VEGFR-1 gene encodes for both the full-length receptor and a soluble form. sVEGFR-1 carries 6 Ig-like domains as well as a 31-amino-acid stretch derived from intron 13.[6] sVEGFR-1 can be distinguished from the other angiogenesis inhibitors because of its specific activity. It is able to bind specifically VEGF-A as well as VEGF-B and PlGF with high affinities, and functions as a decoy receptor by sequestering them.[6] sVEGFR1 cannot inhibit angiogenesis stimulated by other angiogenic factors such as fibroblast growth factor 2 (FGF-2) or hepatocyte growth factor (HGF) because of its binding specificity. The regulation of the expression of sVEGFR-1 is yet to be characterized.

VEGI is a novel member of the tumor necrosis factor (TNF) family identified from the human umbilical vein endothelial cell (HUVECs) cDNA library.[7] VEGI is a type II

Original received August 21, 2006; final version accepted October 5, 2006.

From the Department of Vascular Biology (Y.S.), Institute of Development, Aging, and Cancer, Tohoku University, Sendai, and the Discovery Research Laboratories (H.S.), Shionogi & Co Ltd, Osaka, Japan.

Correspondence to Yasufumi Sato, Department of Vascular Biology, Institute of Development, Aging, and Cancer, Tohoku University, 4-1 Seiryo-machi, Aoba-ku, Sendai 980-8575, Japan. E-mail y-sato@idac.tohoku.ac.jp

Arterioscler Thromb Vasc Biol. **is available at http://www.atvbaha.org** **DOI: 10.1161/01.ATV.0000252062.48280.61**

transmembrane protein composed of 174 amino acid residues. Unlike other members of the TNF family, VEGI is expressed predominantly in ECs,[7] but importantly, the effect of VEGI is not selective to ECs, and inhibits proliferation of various caner cells as well.[8] The expression of VEGI is regulated mainly by transcription factor NF-κB in parallel with other inflammatory cytokines.[9]

DSCR1 and vasohibin are VEGF-inducible molecules in ECs.[10] DSCR1 is a cytoplasmic protein and is shown to act as an endogenous calcineurin inhibitor,[11] and because of this property, DSCR1 is thought to inhibit angiogenesis.[12] Indeed, overexpression of DSCR1 in ECs inhibited angiogenesis.[13] However, our analysis revealed that specific knockdown of DSCR1 in ECs inhibited angiogenesis.[14] Moreover, our subsequent analysis showed that DSCR1 bind not calcineurin but also Raf-1.[15] Thus, the role of DSCR1 in angiogenesis may not be simple.

Vasohibin and its homologue vasohibin-2 are the most recently identified angiogenesis inhibitors.[16,17] This review will focus on the vasohibin family, a negative regulatory system of angiogenesis genetically programmed in endothelial cells.

Vasohibin

Isolation

DNA microarray analysis was used to identify VEGF-inducible genes in ECs.[10] Among 7267 human sequences, 97 were induced more than 2-fold by VEGF stimulation in HUVECs at the 24 hour time point. Of these 97 sequences, 11 were uncharacterized in terms of their biological function, and we could isolate 1 of these11 genes that had antiangiogenic activity, and named it vasohibin.[16] Human vasohibin protein is composed of 365 amino acid residues, without any detectable glycosilation. A cluster of basic amino acids was present in the C-terminal region, but neither a classical secretion signal sequence nor any other functional motif was found among these amino acid sequences by the database search. The lack of classical signal sequence suggests that vasohibin is an unconventional secretory protein.

Initially the antiangiogenic activity of vasohibin was shown using the in vitro Matrigel assay.[16] Recombinant vasohibin protein inhibited the spontaneously formed network-like structures of HUVECs when plated on Matrigel. The antiangiogenic activity of vasohibin was then further determined by 3 independent in vivo assays When matrigel mixed with VEGF with or without vasohibin protein was inoculated subcutaneously to mice, vasohibin inhibited the VEGF-stimulated angiogenesis. However, vasohibin did not inhibit phosphorylation of VEGFRs in HUVECs.[16] Moreover, the "Miles assay" revealed that vasohibin exhibited no inhibitory effect on VEGF-stimulated acute vascular permeability (unpublished observation, 2005). Indicating that vasohibin is not merely an antagonist of VEGF.

When vasohibin was applied to pellets containing fibroblast growth factor (FGF)-2 in a mouse corneal micropocket assay, vasohibin inhibited FGF-2–stimulated angiogenesis.[16] Introduction of the vasohibin gene into a replication-defective adenovirus vector, and applied it to chicken chorioallantoic membrane (CAM) assay, the adenovirus vector encoding vasohibin abrogated the vessel formation whereas the control adenovirus vector encoding β-galactosidase (AdLacZ) did not.[16] All these data implicate that the antiangiogenic effect of vasohibin is not restricted to VEGF-stimulated angiogenesis. The mechanism as to how vasohibin inhibits angiogenesis remains to be elucidated.

Expression Profile

The expression profile of vasohibin was examined in both in vitro and in vivo. In vitro, vasohibin was predominantly expressed in ECs. The expression in ECs was induced not only by VEGF but also by FGF-2. However, human aortic smooth muscle cells (HASMCs) expressed vasohibin weakly, and platelet derived growth factor (PDGF) modestly increased its expression. In addition, fibroblasts did express very low levels of vasohibin, but was unresponsive to the FGF-2 stimulation. Vasohibin expression was not observed in keratinocytes under either basal or EGF-stimulated conditions.[16]

Inflammation often associates pathological angiogenesis. Our analysis revealed that inflammatory cytokines such as TNFα, interleukin (IL)-1β, and interferon (IFN)γ reduced the VEGF-induced expression of vasohibin in ECs.[16,18] The effect of IL-1β was comparable to that of TNFα, whereas the effect of IFNγ was less pronounced. Hypoxia is known to act as a trigger of both physiological and pathological angiogenesis by inducing VEGF. Hypoxia did not affect the basal expression of vasohibin in ECs. However, hypoxia did inhibit the VEGF-stimulated vasohibin mRNA expression, as well as vasohibin protein synthesis in ECs.[16]

Northern blot analysis of the samples from various tissues revealed that vasohibin was expressed in the brain, and to a lesser extent, in the heart and kidney in the adult.[16] Moreover, a robust expression of vasohibin was demonstrated in the placenta and various developing organs of the human embryo.[16] Furthermore, immunohistochemical analysis revealed that vasohibin was present only in ECs of the human placenta and developing organs in embryo.[16,17] Thus vasohibin is thought to be a molecule selectively expressed in ECs during angiogenesis.

Signals for the Induction of Vasohibin in ECs

The intracellular signaling for the induction of vasohibin in HUVECs by VEGF was characterized using blocking anti-VEGFRs mAbs to test which receptor was involved in the induction of vasohibin.[18] Anti–VEGFR-2 antibodies but not anti–VEGFR-1 antibodies inhibited the VEGF-stimulated induction of vasohibin. The downstream intracellular signaling pathways of VEGFR-2 for the induction of vasohibin were further investigated. GF109203X, a broad-spectrum inhibitor of protein kinase C (PKC), strongly inhibited the increase of vasohibin mRNA and protein in response to VEGF, which was in line with the observation that Phorbol 12-myristate 13-acetate (PMA), an activator of PKC, enhanced the expression of vasohibin in HUVECs. Selective PKC isoform inhibitors were used to clarify which PKC isoforms were involved in the upregulation of vasohibin. Rottlerin, a specific inhibitor of PKCδ, completely blocked

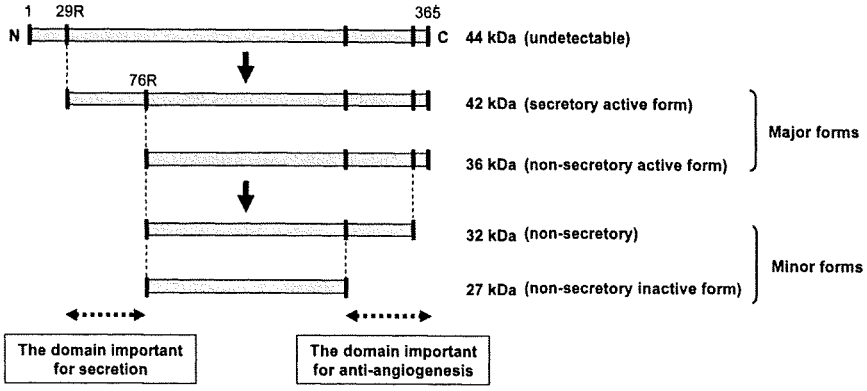

Figure 1. Posttranslational processing, secretion, and biological activity of vasohibin-1. Forty-four-kDa full-length vasohibin-1 cannot be detected. Four different forms of vasohibin-1 are generated after the translation. Forty-two-kDa vasohibin-1 is the major secretory form with antiangiogenic activity. N terminus region is important for secretion, whereas C terminus region is important for antiangiogenesis. The antiangiogenic activity of 32-kDa form is not determined.

the upregulation of vasohibin, whereas Gö6976, a specific inhibitor of PKCα, and HBDDE, an inhibitor of PKCα and PKCγ, partially inhibited it. Hispidin, a specific inhibitor of PKCβ, did not affect the upregulation of vasohibin.[18] From these results it is concluded that PKCδ transduced a principal signal for the upregulation of vasohibin through VEGF. FGF-2 increased the expression of vasohibin in ECs to a level comparable to that obtained with VEGF, and rottlerin again completely blocked FGF-2–stimulated upregulation of vasohibin.[18] Accordingly, the principal signaling pathways for the induction of vasohibin by 2 representative angiogenic growth factors considerably overlap. PKC-δ is known to be a transducer of antiangiogenic signals in ECs.[19] Thus, vasohibin can be a downstream effecter of PKC-δ in ECs for angiogenesis inhibition.

Actinnomycin D treatment did not change the decay of VEGF-induced vasohibin mRNA.[18] Thus, the increase of vasohibin mRNA by VEGF is not determined by mRNA stability. However, when cycloheximide was added, the expression of vasohibin mRNA was completely abolished in both basal and VEGF-stimulated condition.[18] Thus, de novo protein synthesis is indispensable for the induction of vasohibin mRNA.

Posttranslational Processing, Secretion, and Biological Activity

To understand the posttranslational modification of vasohibin protein, vasohibin cDNA was overexpressed in ECs.[20] The calculated vasohibin protein is 44 kDa. When the retroviral vector encoding human vasohibin cDNA was transfected to the HUVEC-derived HUV-SV8 cells, 2 major (42, 36 kDa) bands and 2 minor (32, 27 kDa) bands were detected in their cellular extract, whereas 42 kDa product was detected in the conditioned medium. Because the 44 kDa complete from was not seen, amino terminal region is thought to be processed simultaneously or immediately after the translation. To characterize the structures of these multiple forms of vasohibin proteins, various vasohibin cDNA mutants were generated to substitute some basic amino acids. This analysis revealed that there were 2 cleaving sites in the amino terminal region; arginine 29 and arginine 76. The 42 kDa form is generated by the cleavage at arginine 29, whereas the 36 kDa form is generated by the cleavage at arginine 76. Because only 42 kDa vasohibin was shown in the conditioned medium, the domain from arginine 29 to arginine 76 is thought to be important for the secretion. The mechanism of its secretion is not known at present. Cleaving sites in the carboxyl terminal region are not determined yet. However, because the calculated molecular weight of the vasohibin protein from methionine 77 to carboxyl terminal end is 33 kDa, the carboxyl terminal of the 32 kDa form should be very close to the end. From the calculation of the molecular weight, the 27 kDa form may lack about 47 amino acids from the carboxyl terminal, and this lacked region contains the cluster of basic amino acids (Figure 1).

To determine the biological function of these processed forms of vasohibin, mouse corneal micropocket assay was used to check for antiangiogenic activities using purified recombinant proteins for Vh(77–365) and Vh(77–318).[20] Vh(77–365) inhibited FGF-2–induced angiogenesis, suggesting that truncation of the 76 amino terminal residues does not influence antiangiogenic activity of vasohibin. On the other hand, Vh(77–318) could not exert antiangiogenic activity, suggesting that the carboxyl terminal is essential for antiangiogenic activity (Figure 1).

Application to Antiangiogenic Therapy

Because vasohibin is identified as a novel angiogenesis inhibitor, one may anticipate the application of vasohibin to antiangiogenic therapy. We have examined the effect of vasohibin on 3 different states of pathological angiogenesis: tumor angiogenesis, arterial adventitial angiogenesis, and retinal angiogenesis.

For tumor angiogenesis, we transfected human vasohibin cDNA into Lewis lung carcinoma (LLC) cells, establishing two permanent human vasohibin-producing clones.[16] Vasohibin cDNA transfection did not alter the proliferation of LLC cells in vitro. To show the effect of vasohibin produced by LLC cells on ECs, mock or vasohibin-transfected LLC cells were plated on the lower compartment of modified Boyden chambers, and the migration of HUVECs toward LLC cells was analyzed. The number of migrated HUVECs was significantly reduced when vasohibin-transfected LLC cells were plated on the lower chamber. Then LLC cells were inoculated intradermally in mice, and the growth of tumor was observed. The growth of vasohibin producing LLC cells in mice was significantly retarded, and immunohistological analysis of CD31 revealed that tumors of mock-transfectants contained large luminal vessels whereas those of vasohibin

producing LLC cells contained very small ones, even when the size of tumors did not differ dramatically.[16]

It has been documented that the extent of adventitial angiogenesis from vasa vasora correlates with atherosclerosis.[21] Arterial neointimal formation was investigated using the mouse cuff model.[22] In this model, cuff placement around the femoral artery does not denudate luminal endothelium, but induces adventitial angiogenesis, and that causes neointimal formation. To apply vasohibin protein to mice, we injected replication-defective adenovirus vectors encoding human vasohibin gene (AdVh) to mice via the tail vein. In this way, vasohibin was synthesized in the liver, secreted in the plasma, and was able to exhibit antiangiogenic activity in the remote sites after the delivery through systemic circulation.[22] We observed that adventitial angiogenesis and neointimal formation were significantly inhibited in AdVh-injected mice in this model. Thus, vasohibin is thought to play a preventive role in angiogenesis-dependent neointimal formation.

Retinal angiogenesis is the major cause of acquired blindness.[23] The mouse model of retinopathy of premature (ROP) is a useful model to study the hypoxia-induced regulation of VEGF expression.[24] In this model, placement of neonatal mice into a high oxygen environment results in decreased expression of VEGF and regression of newly developed retinal blood vessels. When mice are returned to room air, the poorly vascularized retina becomes hypoxic and VEGF is induced, which causes retinal angiogenesis. Interestingly, when endogenous vasohibin expression in the retinal vessels was knocked down by siRNA, retinal angiogenesis was augmented.[25] This result indicates that endogenous vasohibin plays a role in the inhibition of angiogenesis. However, it is assumed that the extent of endogenous vasohibin expression is not enough to control retinal angiogenesis. To determine the effect of exogenous vasohibin, we used AdVh or recombinant vasohibin protein. Intraocular injection of recombinant vasohibin or AdVh strongly suppressed retinal angiogenesis.[25]

A Homologue of Vasohibin and Splicing Variants

By the search of DNA sequences in the database, a homologous gene was found. This gene was named vasohibin-2, and the prototype vasohibin as renamed vasohibin-1.[17] Human vasohibin-2 is composed of 355 amino acid residues, and also exhibits antiangiogenic activity. The overall homology between human vasohibin-1 and vasohibin-2 is 52.5% at the amino acid level. The genes for human vasohibin-1 and vasohibin-2 are located on chromosome 14q24.3 and 1q32.3, respectively.

So far 8 exons for the vasohibin-1 gene and 11 exons for the vasohibin-2 gene have been shown in Ensembl human genome database to form multiple transcripts for these paralogous genes owing to alternative splicing (Figure 2). Prototype full-length vasohibin-1 is composed with 5589 bp consisting of 8 exons, and will receive posttranslational processing as described previously. In addition, two splicing variants of 522 bp and 1459 bp have been registered in the database. Although open reading frames encoding 42 and 204 amino acids, respectively, exists in these transcripts and the expression of all three splicing variants are confirmed by real-time polymerase chain reaction using unique primers (unpublished observation, 2006), the biological significance

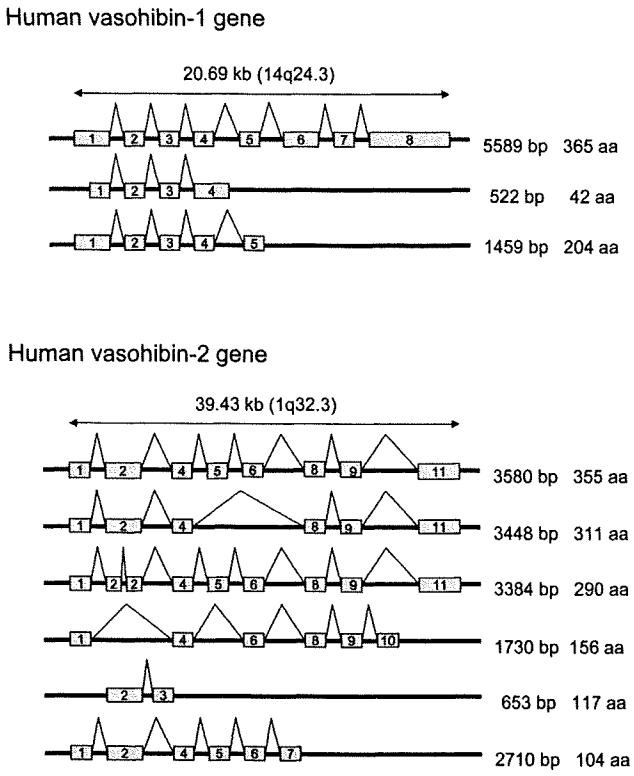

Figure 2. Schematic representation of human vasohibin-1 and -2 genomic structures and splicing patterns. Exons of human vasohibin-1 and vasohibin-2 genes are numbered in their orders on the chromosomes. Length of each transcript (bp) and polypeptides encoded in each transcript (aa) are shown in the right side of each splicing pattern.

of the 2 shorter variants have not been clarified yet. No alternative splicing for the mouse vasohibin-1 gene has been reported.

We have recently described the existence of 3 splicing variants for human vasohibin-2 transcripts, which encode polypeptides of 290, 311, and 355 amino acids.[17] Eight exons are joined to generate the variant of 355 amino acids, and this isoform is predominantly expressed in HUVECs. The isoform consisting of 290 amino acids has been confirmed to have antiangiogenic activity. In addition to those 8 exons, 3 additional exons are now found in Ensembl database generating 3 small different splicing variants encoding polypeptides of 104, 117, and 156 amino acids. The biological significance of these shorter variants have not been clarified yet. In the mouse genome, vasohibin-1 gene is located at 12D2 spanning 13.39 kb and consisting of 7 exons. Mouse vasohibin-2 gene is located at chromosome 1H6 spanning 31.48 kb and single splicing pattern with 8 exons is reported in Ensembl database.

Whereas the expression of vasohibin-2 was compared with that of vasohibin-1, vasohibin-2 expression in cultured endothelial cells was low and not inducible by the stimulation that induced vasohibin-1. However, the expression pattern of vasohibin-2 in vivo resembled to that of vasohibin-1.[17] Immunohistochemical analysis revealed that vasohibin-1 and vasohibin-2 were diffusely expressed in ECs in embryonic organs during midgestation. After that time point,

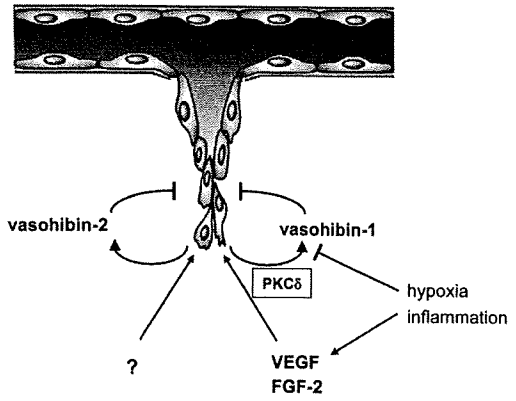

Figure 3. The role of vasohibin family in the regulation of angiogenesis. Vasohibin-1 and vasohibin-2 form a novel family of angiogenesis inhibitors genetically programmed in ECs. Vasohibin-1 is induced in ECs by VEGF and FGF-2. Hypoxia and inflammatory cytokines, which induce VEGF, may abort the expression of vasohibin-1 in ECs. The mechanism for the regulation of vasohibin-2 expression is not known.

vasohibin-1 and vasohibin-2 became faint, but persisted to a certain extent in arterial ECs from late-gestation to neonate. Interestingly, expression of vasohibin-1 and vasohibin-2 could be augmented in vivo by the local expression with the VEGF gene in the embryonic brain, or by cutaneous wounding in adult mice.[17]

Concluding Remarks

A summary of the vasohibin family is shown in Figure 3. Negative feedback regulation is one of the most important physiological mechanisms, and has been demonstrated to control a wide range of phenomena. However, very few endothelium-derived negative feedback regulators have been established for the regulation of angiogenesis. Vasohibin-1 is the first secretory antiangiogenic factor induced by VEGF in ECs. We would like to propose that vasohibin-1 has the property of negative feedback regulator of angiogenesis. Thus far Vasohibin-2 is a sole homologue of vasohibin-1, which exhibits antiangiogenic activity as well. Although vasohibin-2 lacks the property of VEGF or FGF-2 inducibility in vitro, its expression pattern is resemble to that of vasohibin-1. Thus, vasohibin-1 and vasohibin-2 form a novel family of angiogenesis inhibitors genetically programmed in ECs. The discovery of vasohibin family should shed light on the novel genomic basis of the negative regulation of angiogenesis.

Acknowledgments

We thank Dr Pieter Koolwijk at VU University Medical Center for valuable comments on this manuscript.

Disclosures

None.

References

1. Risau W. Mechanisms of angiogenesis. *Nature.* 1997;386:671–674.
2. Ferrara N. Vascular endothelial growth factor: basic science and clinical progress. *Endocr Rev.* 2004;25:581–611.
3. Eklund L, Olsen BR. Tie receptors and their angiopoietin ligands are context-dependent regulators of vascular remodeling. *Exp Cell Res.* 2006; 312:630–641.
4. Lee HJ, Cho CH, Hwang SJ, Choi HH, Kim KT, Ahn SY, Kim JH, Oh JL, Lee GM, Koh GY. Biological characterization of angiopoietin-3 and angiopoietin-4. *FASEB J.* 2004;18:1200–1208.
5. Sato Y. Update on endogenous inhibitors of angiogenesis. *Endothelium.* 2006;13:147–155.
6. Yamaguchi S, Iwata K, Shibuya M. Soluble Flt-1 (soluble VEGFR-1), a potent natural antiangiogenic molecule in mammals, is phylogenetically conserved in avians. *Biochem Biophys Res Commun.* 2002;291:554–559.
7. Zhai Y, Ni J, Jiang GW, Lu J, Xing L, Lincoln C, Carter KC, Janat F, Kozak D, Xu S, Rojas L, Aggarwal BB, Ruben S, Li LY, Gentz R, Yu GL. VEGI, a novel cytokine of the tumor necrosis factor family, is an angiogenesis inhibitor that suppresses the growth of colon carcinomas in vivo. *FASEB J.* 1999;13:181–189.
8. Haridas V, Shrivastava A, Su J, Yu GL, Ni J, Liu D, Chen SF, Ni Y, Ruben SM, Gentz R, Aggarwal BB. VEGI, a new member of the TNF family activates nuclear factor-kappa B and c-Jun N-terminal kinase and modulates cell growth. *Oncogene.* 1999;18:6496–6504.
9. Xiao Q, Hsu CY, Chen H, Ma X, Xu J, Lee JM. Characterization of cis-regulatory elements of the vascular endothelial growth inhibitor gene promoter. *Biochem J.* 2005;388:913–920.
10. Abe M, Sato Y. cDNA microarray analysis of the gene expression profile of VEGF-activated human umbilical vein endothelial cells. *Angiogenesis.* 2001;4:289–298.
11. Fuentes JJ, Genesca L, Kingsbury TJ, Cunningham KW, Perez-Riba M, Estivill X, de la Luna S. DSCR1, overexpressed in Down syndrome, is an inhibitor of calcineurin-mediated signaling pathways. *Hum Mol Genet.* 2000;9:1681–1690.
12. Yao YG, Duh EJ. VEGF selectively induces Down syndrome critical region 1 gene expression in endothelial cells: a mechanism for feedback regulation of angiogenesis? *Biochem Biophys Res Commun.* 2004;321:648–656.
13. Minami T, Horiuchi K, Miura M, Abid MR, Takabe W, Noguchi N, Kohro T, Ge X, Aburatani H, Hamakubo T, Kodama T, Aird WC. Vascular endothelial growth factor- and thrombin-induced termination factor, Down syndrome critical region-1, attenuates endothelial cell proliferation and angiogenesis. *J Biol Chem.* 2004;279:50537–50554.
14. Iizuka M, Abe M, Shiiba K, Sasaki I, Sato Y. Down syndrome candidate region 1 (DSCR1), a downstream target of VEGF in endothelial cells, regulates cell migration and angiogenesis via the functional interaction with integrin $\alpha v\beta 3$. *J Vasc Res.* 2004;41:334–344.
15. Cho Y-J, Abe M, Kim SY, Sato Y. Raf-1 is a binding partner of DSCR1. *Arch Biochem Biophys.* 2005;439:121–128.
16. Watanabe K, Hasegawa Y, Yamashita H, Shimizu K, Ding Y, Abe M, Ohta H, Imagawa K, Hojo K, Maki H, Sonoda H, Sato Y. Vasohibin as an endothelium-derived negative feedback regulator of angiogenesis *J Clin Invest.* 2004;114:898–907.
17. Shibuya T, Watanabe K, Yamashita H, Shimizu K, Miyashita H, Abe M, Moriya T, Ohta H, Sonoda H, Shimosegawa T, Tabayashi K, Sato Y. Isolation of vasohibin-2 as a sole homologue of VEGF-inducible endothelium-derived angiogenesis inhibitor vasohibin: a comparative study on their expressions. *Arterioscl Thromb Vasc Biol.* 2006;26:1051–1057.
18. Shimizu K, Watanabe K, Yamashita H, Abe M. Yoshimatsu H, Ohta H, Sonoda H, Sato Y. Gene regulation of a novel angiogenesis inhibitor, vasohibin, in endothelial cells. *Biochem Biophys Res Commun.* 2005;327:700–706.
19. Harrington EO, Loffler J, Nelson PR, Kent KC, Simons M, Ware JA. Enhancement of migration by protein kinase Calpha and inhibition of proliferation and cell cycle progression by protein kinase Cdelta in capillary endothelial cells. *J Biol Chem.* 1997;272:7390–7397.
20. Sonoda H, Ohta H, Watanabe K, Yamashita H, Kimura H, Sato Y. Multiple processing forms and their biological activities of a novel angiogenesis inhibitor vasohibin. *Biochem Biophys Res Commun.* 2006;342:640–646.
21. Fleiner M, Kummer M, Mirlacher M, Sauter G, Cathomas G, Krapf R, Biedermann BC. Arterial neovascularization and inflammation in vulnerable patients: early and late signs of symptomatic atherosclerosis. *Circulation.* 2004;110:2843–2850.
22. Yamashita H, Abe M, Watanabe K, Shimizu K, Moriya T, Sato A, Satomi S, Ohta H, Sonoda H, Sato Y. Vasohibin prevents arterial neointimal formation through angiogenesis inhibition. *Biochem Biophys Res Commun.* 2006;345:919–925.
23. Campochiaro PA. Ocular neovascularisation and excessive vascular permeability. *Expert Opin Biol Ther.* 2004;4:1395–1402.
24. Campochiaro PA, Hackett SF. Ocular neovascularization: a valuable model system. *Oncogene.* 2003;22:6537–6548.
25. Shen JK, Yang XR, Sato Y, and Campochiaro PA. Vasohibin is Up-regulated by VEGF in the Retina and Suppresses VEGF receptor 2 and Retinal Neovascularization. *FASEB J.* 2006;20:723–725.

EphB4 Overexpression in B16 Melanoma Cells Affects Arterial-Venous Patterning in Tumor Angiogenesis

Xiaoyong Huang,[1,2] Yoshihiro Yamada,[2] Hiroyasu Kidoya,[2] Hisamichi Naito,[2] Yumi Nagahama,[2] Lingyu Kong,[2] Shin-Ya Katoh,[2] Weng-lin Li,[1] Masaya Ueno,[2] and Nobuyuki Takakura[2]

[1]Department of Stem Cell Biology, Cancer Research Institute, Kanazawa University, Kanazawa, Japan and [2]Department of Signal Transduction, Research Institute for Microbial Diseases, Osaka University, Suita-shi, Osaka, Japan

Abstract

EphB4 receptor and its ligand ephrinB2 play an important role in vascular development during embryogenesis. In blood vessels, ephrinB2 is expressed in arterial endothelial cells (EC) and mesenchymal supporting cells, whereas EphB4 is only expressed in venous ECs. Previously, we reported that OP9 stromal cells, which support the development of both arterial and venous ECs, in which EphB4 was overexpressed, could inhibit ephrinB2-positive (ephrinB2$^+$) EC development in an embryonic tissue organ culture system. Although the EphB4 receptor is expressed in a variety of tumor cells, its exact function in regulating tumor progression has not been clearly shown. Here we found that overexpression of EphB4 in B16 melanoma cells suppressed tumor growth in a s.c. transplantation tumor model. Histologic examination of these tumors revealed that EphB4 overexpression in B16 cells selectively suppressed arterial ephrinB2$^+$ EC development. By coculturing ephrinB2-expressing SV40-transformed mouse ECs (SVEC) with EphB4-overexpressing B16 cells, we found that EphB4 induced the apoptosis of SVECs. However, ephrinB2 did not induce the apoptosis of EphB4-overexpressing B16 cells. Based on results from these experiments, we concluded that EphB4 overexpression in B16 tumor cells suppresses the survival of arterial ECs in tumors by a reverse signaling via ephrinB2. [Cancer Res 2007;67(20):9800–8]

Introduction

The growth of solid tumors is closely associated with the ability to recruit blood vessels, which can supply tumors with the growth factors, oxygen, and nutrients necessary for their survival and growth and for the maintenance of the malignant state. In embryos, blood vessels are initially formed by a process called vasculogenesis but become remodeled and mature through a second process called angiogenesis, which results in the development of a highly hierarchical architecture of blood vessels ranging from small to large (1). During these processes, a distinction develops between arterial and venous endothelial cells (EC); eventually, the arterial ECs selectively express ephrinB2 and the venous ECs preferentially express EphB4, which is a cognate receptor tyrosine kinase for ephrinB2 (2–4).

Eph receptors and ephrins are frequently expressed in reciprocal patterns that correlate with cellular boundaries during embryonic development (5). Consistent with this expression pattern, Eph-ephrin signaling regulates the boundary of distinct cells in culture (6) and is required for vascular modeling (2, 7), axon guidance (8, 9), and epithelial-mesenchymal transitions (10). Reciprocal expression of ephrinB2 and EphB4 in arterial and venous ECs, respectively, suggests that ephrinB2 and EphB4 might interact at the arterial-venous interface and regulate angiogenesis (2–4). Targeted disruption of either ephrinB2 or EphB4 in mice has been shown to lead to early embryonic lethality through the disruption of blood vessel formation in angiogenesis but not in vasculogenesis (2–4). EphrinB2 contains transmembrane and cytoplasmic domains; therefore, it has been suggested that the functioning of this receptor/ligand system is dependent on cell-to-cell contact (5). EphB4 is a member of the receptor tyrosine kinase family and initiates signal transduction through autophosphorylation after ligand binding (forward signaling); however, in contrast to other soluble ligands for receptor system, ephrinB2 also has the ability to initiate receptor-like active signaling (reverse signaling; refs. 5, 11, 12). Indeed, a loss-of-function experiment, in which the cytoplasmic domain of ephrinB2 was deleted, showed that bidirectional EphB4/ephrinB2 signaling was required for proper arterial and venous development (13).

It was originally assumed that the blood vessel system in tumors was composed of homogeneous capillaries, based on their uniformly small size and the sparse adhesion of mural cells to ECs. However, it has been reported that the vessels in tumors can be divided into ephrinB2-positive (ephrinB2$^+$) arterial and ephrinB2-negative (ephrinB2$^-$), and therefore presumably, venous ones (7). This suggests that the EphB4/ephrinB2 system is involved in tumor angiogenesis and that it may have an affect on the specification of arteries and veins in the tumor environment. Moreover, EphB4 expression has been reported in numerous tumors such as breast, liver, gastrointestinal, prostate, bladder, lung, and ovarian cancers, as well as leukemia, mesothelioma, and melanoma (14–19). Recent research reported that reduction of EphB4 activity accelerated tumorigenesis in the colon and rectum and that loss of EphB4 expression represented a critical step in colorectal cancer progression (15). Furthermore, a highly significant correlation was reported between EphB4 positivity and low histologic grading of tumor cells in breast cancer (20). Other reports also showed that overexpression of EphB4 is inversely related to a poor prognosis in head and neck squamous cell carcinoma and endometrial carcinoma (21, 22). These results indicated that EphB4 expression is not compatible with tumor progression. However, in mesothelioma, up-regulation of EphB4 was shown to provide a survival advantage in tumor tissue (17)

Note: Supplementary data for this article are available at Cancer Research Online (http://cancerres.aacrjournals.org/).

Requests for reprints: Nobuyuki Takakura, Department of Signal Transduction, Research Institute for Microbial Diseases, Osaka University, 3-1 Yamada-oka, Suita, Osaka 565-0871, Japan. Phone: 81-6-6879-8316; Fax: 81-6-6879-8314; E-mail: ntakaku@biken.osaka-u.ac.jp.

doi:10.1158/0008-5472.CAN-07-0531

and resulted in growth of the tumor. At present, little is known about this apparent discrepancy in terms of the function of EphB4 in tumor progression, but it is possible that coexpression of another member of the EphB family, such as EphB1, EphB2, EphB3, and EphB6, or coexpression of EphB4 ligands such as ephrinB2 in tumor cells may affect tumor cell viability and proliferation. Indeed, it was reported that, in mesothelioma, ephrinB2 and EphB4 were almost exclusively coexpressed in cells from tumor cell lines and primary cancers, and that knockdown of either ephrinB2 or EphB4 by small interfering RNA inhibited the viability of tumor cells coexpressing EphB4/ephrinB2 (17). This suggested that the expression of ephrinB2 in tumor cells has a reciprocal affect on EphB4 expression in an autocrine or paracrine manner. Similar coexpression of this receptor-ligand pair has been reported in other tumor types, including endometrial, lung, and colon carcinoma, both in the corresponding tumor cell lines and primary cancers (16, 23, 24).

Although the expression of EphB4 in various tumors and its effect on tumor progression have been reported, its other role in the development of arteries and veins in tumors has not been clarified. To investigate this, we searched for tumor cells that expressed EphB4 on their surface, but not ephrinB2, to exclude any autocrine or paracrine effects of EphB4 on tumor cells. Furthermore, we looked for murine tumor cell lines because of the availability of an *in vivo* tumor angiogenesis model, in which murine EphB4 affects murine ephrinB2 of ECs. Among tumor cell lines tested, such as melanoma, colon cancer, lung cancer, and mammary gland tumor, we found a B16 mouse melanoma cell line that matched these criteria. Using this cell line, we overexpressed or knocked down EphB4 and observed the effect of EphB4 on blood vessel formation and tumor growth. Moreover, to test the viability of ephrinB2$^+$ ECs on stimulation with EphB4$^+$ tumor cells, we cocultured an ephrinB2-induced EC line, a SV40-transformed mouse EC line (SVEC; ref. 25), with B16 melanoma cells *in vitro*, and observed dose dependency of cell-surface EphB4 and apoptosis of ephrinB2$^+$ ECs.

Materials and Methods

Animals. C57BL/6 mice and Wistar rats were purchased from Japan SLC at 8 weeks of age and used between 8 and 12 weeks of age. EphB4$^{LacZ/+}$ and ephrinB2$^{LacZ/+}$ mice (2, 4) were provided by Dr. D.J. Anderson (California Institute of Technology, Pasadena, CA). Animal care in our laboratory was in accordance with the guidelines of Kanazawa and Osaka University for animal and recombinant DNA experiments.

Cell lines and transfection. B16 (mouse melanoma) cells were cultured in DMEM supplemented with 10% FCS. BaF3 pre-B hematopoietic cells were cultured in RPMI 1640 supplemented with 10% FCS and 1 ng/mL interleukin-3.

Transfection of mouse full-length *EphB4* or *ephrinB2* cDNA (26) was done using Lipofectamine Plus reagent (Invitrogen). Stable transfection was obtained by antibiotic resistance selection using G418 (Life Technologies, Inc.). Stable knockdown of *EphB4* gene in B16 cells was done using the short hairpin RNA (shRNA) method. shRNA coding for *EphB4* was introduced into the pSINsi-hU6 DNA vector (Takara) at the *Bam*H1 and *Cla*1 ligation sites according to the manufacturer's instruction. shRNA oligonucleotides were synthesized corresponding to the published sequence of *EphB4* mRNA (NM_010144). The insert for *EphB4* shRNA (forward strand, 5′-GCATCACAGTCAGACTCAACT-3′; reverse strand, 5′-AGTTGAGTCTGACTGTGATGC-3′) and a nonspecific oligonucleotide insert for negative control (forward strand, 5′-gatccGATCGTTGGTGTGGTGGGTCGttcaagagaACTACCATGCTCCCATGAACAttttttat-3′; reverse strand, 5′-cgataaaaaaTGTTCATGGGAGCATGGTAGTtctcttgaaCGACCCACCACACCAACGATCg-3′) were used. Plasmids were transfected into B16 by electroporation (Amaxa Biosystems); 48 h after electroporation, the cells were harvested by trypsin-EDTA (Life Technologies) and reseeded at a density of 2×10^4 cells in 10-cm culture dishes. The following day, geneticine (Life Technologies) was added to a final concentration of 1,000 μg/mL. Eight days after addition of geneticine, colonies were picked with a cloning ring (Asahi Techno Glass) and reseeded in the culture plate. For the evaluation of *EphB4* knockdown, *EphB4* expression was determined by real-time reverse transcription and reverse transcription-PCR (RT-PCR).

RT-PCR analysis. Total RNA was extracted from cells using the RNeasy plus mini kit (Qiagen) according to the manufacturer's protocol. Total RNA was reverse transcribed into cDNA using Exscript RT Reagent Kit (Takara). Primer pairs for studying the expression of mouse *EphB4*, mouse *ephrinB2*, human *EphB4*, human *ephrinB2*, mouse *β-actin*, or human *glyseraldehyde-3-phosphate dehydrogenase* (*GAPDH*) were, for real-time PCR, *EphB4* (sense, 5′-AATGTCACCACTGACCGTGA-3′; antisense, 5′-TCAGGAAACGAACACTGCTG-3′) and *GAPDH* (sense, 5′-TGGCAAAGTGGAGATTGTTGCC-3′; antisense, 5′-AAGATGGTGATGGGCTTCCCG-3′), and for RT-PCR primers, mouse *EphB4* (sense, 5′-CGTCCTGATGTCACCTATACCTTTGAGG-3′; antisense, 5′-GAGTACTCAACTTCCCTCCCATTGCTCT-3′), mouse *ephrinB2* (sense, 5′-AGGAATCACGGTCCAACAAG-3′; antisense, 5′-GTCTCCTGCGGTACTTGAGC-3′), human *EphB4* (sense, 5′-GGCTGCTCGCAACATCCTAGT-3′; antisense, 5′-CCACATCACAATCCCGTAAC-3′), human *ephrinB2* (sense, 5′-CTGCTGGATCAACCAGGAAT-3′; antisense, 5′-GATGTTGTTCCCCGAATGTC-3′), mouse *β-actin* (sense, 5′-CCTAAGGCCAACCGTGAAAAG-3′; antisense, 5′-TCTTCATGGTGCTAGGAGCCA-3′), and human *GAPDH* (sense, 5′-GAAGGTGAAGGTCGGAGTC-3′; antisense, 5′-GAAGATGGTGATGGGATTTC-3′). Real-time PCR analysis was done with Platinum SYBR Green qPCR SuperMix-UDG (Invitrogen). The levels of PCR products were monitored with an ABI PRISM 7900HT sequence detection system and analyzed with ABI PRISM 7900 SDS software (Applied Biosystems). The adjustment of baseline and threshold was done according to the manufacturer's instructions. The relative abundance of transcripts was normalized to the constitutive expression level of *GAPDH* RNA.

Generation of EphB4 monoclonal antibody. The extracellular ligand binding domain of mouse *EphB4* (amino acids 39–165) was cloned into pGEX-2T to generate glutathione *S*-transferase (GST)–fused protein. EphB4 ligand binding domain expressed as a GST fusion protein in DH5α *E. coli* was purified by affinity chromatography and used as an immunogen for Wistar rats. The methods for generation of hybridoma cells using X63Ag8 mouse myeloma cells and the purification of monoclonal antibody (mAb) were the same as previously described (27). The sensitivity of the mAb produced from the hybridoma clone (VEB4-7E4) was confirmed by Western blotting and fluorescence-activated cell sorting (FACS) analysis with BaF3 cells stably transfected with EphB4 (BaF3/EphB4). Furthermore, by immunohistochemistry, the specificity of the mAb was examined by reciprocal expression of ephrinB2 and EphB4 or colocalization of ECs stained with anti–β-galactosidase and anti-EphB4 antibody on the hind limb section of ephrinB2$^{Lac/+}$ or EphB4$^{Lac/+}$ mice, respectively.

Immunoprecipitation and Western blotting. Cells were lysed on ice with lysis buffer [50 mmol/L HEPES (pH 7.4), 1% Triton X-100, 10% glycerol, 10 mmol/L sodium pyrophosphate, 100 mmol/L sodium fluoride, 4 mmol/L EDTA, 2 mmol/L sodium orthovanadate, 50 μg/mL aprotinin, 1 mmol/L phenylmethylsulfonyl fluoride, 100 mmol/L leupeptin, 25 μmol/L pepstatin A]. Cell lysates were cleared by centrifugation for 15 min at 15,000 × *g* at 4°C, and then proteins were subjected to SDS-PAGE and transferred onto polyvinylidene difluoride membranes (Nihon Millipore). Membranes were blocked with 5% normal goat serum, 1% bovine serum albumin, 5% skimmed milk in TBST [20 mmol/L Tris (pH 7.4), 150 mmol/L sodium chloride, 0.1% Tween 20] for 60 min at room temperature. Membranes were washed and then incubated for 60 min at room temperature with anti-EphB4 mAb or anti-ephrinB2 polyclonal antibody (Santa Cruz Biotechnology), followed by 60 min at room temperature with horseradish peroxidase–conjugated goat anti-mouse immunoglobulins (Amersham Pharmacia Biotech) or goat anti-rabbit immunoglobulins antibody (Biosourse). Proteins were visualized by enhanced chemiluminescence detection system (LAS-3000 mini, Fuji).

FACS analysis. Flow cytometric analysis was done as previously described (28). The antibodies used in this experiment were anti-EphB4 mAb (VEB4-7E4) and Alexa Fluor 488 goat anti-rat immunoglobulin G (IgG) (H+L) antibody (Molecular Probes). For the analysis of specific binding of EphB4 mAb to EphB4 on BaF3/EphB4 cells, cells were preincubated with soluble EphB4 receptor (sEphB4; extracellular domain of EphB4 fused with human Fc of IgG; ref. 26) for 30 min on ice. The stained cells were analyzed by FACSCalibur (Becton Dickinson).

Immunohistochemistry. Tissue fixation, preparation of tissue sections, and staining of sections with antibodies were done as previously described (29). Antibodies used in immunohistochemical staining were nonlabeled or FITC-conjugated anti–platelet/endothelial cell adhesion molecule 1 (PECAM-1) mAb (PharMingen), anti–β-galactosidase antibody (Chemicon), and anti-EphB4 mAb (VEB4-7E4). Secondary antibodies used were horseradish peroxidase– or Alexa Fluor 488–conjugated goat anti-rat IgG(H+L) antibody for anti-EphB4 mAb (Biosource) and nonlabeled anti–PECAM-1 mAb or HRP-, alkaline phosphatase–, or Alexa Fluor 546–conjugated goat anti-rabbit IgG antibody (Molecular Probes) for anti–β-galactosidase antibody. Anti–PECAM-1 antibody was developed with HRP-conjugated anti-rat IgG antibody (Biosource). For color reaction of HRP, samples were soaked in PBS containing 250 μg/mL diaminobenzidine (Dojin Chem.) in the presence of 0.05% $NiCl_2$ for 10 min, and 0.01% hydrogen peroxidase was added for the enzymatic reaction. For the color reaction of alkaline phosphatase, new Fuchsin substrate kit (DAKO) was used. Nuclear staining was done with Hoechst (Sigma) or 4′,6-diamidino-2-phenylindole (DAPI; Invitrogen) to obtain fluorescent images. Finally, the sections were observed and photographed under a microscope (IX-70, Olympus) with UV lamp.

***In vitro* proliferation assay.** Cells (10^3 per well) were seeded into 96-well plates and cultured in DMEM supplemented with 10% FCS under 37°C, CO_2 0.5%. The cell number was counted daily.

Mouse xenograft assay. Tumor cells (5×10^6 per mouse in 0.1-mL PBS) were injected s.c. into 8-week-old female wild-type C57BL/6, ephrinB2$^{LacZ/+}$, or EphB4$^{LacZ/+}$ mice, as previously reported (30). Tumor volumes were measured with calipers every 3 days and calculated as width × width × length × 0.52. Tumor tissues were removed from mice on day 18 postinjection.

Coculture system and apoptosis assay. B16/mock (B16 cells induced with mock vector) or B16/EphB4 (B16 cells induced with mouse EphB4 expression vector) tumor cells labeled with PKH26 Red Fluorescent Cell Linker Mini Kit (Sigma) were seeded into 12-well plates in culture medium (DMEM supplemented with 10% FCS). When cells had reached 80% confluency, they were serum starved for 12 h in DMEM. SVECs transduced with mouse ephrinB2 (SVEC/ephrinB2 cells) were prelabeled with PKH67 Green Fluorescent Cell Linker (Sigma) and serum starved for 12 h in DMEM, and then added in medium (DMEM, 2% FCS) either into B16/mock or B16/EphB4 tumor cells or trans-well plates with 0.4-μm pores (Corning, Inc.). For binding inhibition assays of EphB4 in B16/EphB4 cells and ephrinB2 in SVEC/ephrinB2 cells, soluble EphB4-Fc (sEphB4; 5 μg/mL) was added. After 24 h of coculture, cells were harvested from the culture plate using trypsin-EDTA and stained with Annexin V-Cy5 Apoptosis Detection Kit (BioVision) and DAPI (Invitrogen). Stained cells were analyzed by flow cytometry with UV laser (JSAN, Bay bioscience).

Statistical analysis. All date are presented as mean ± SE. For statistical analysis, Microsoft Excel software was used for two-sided Student's *t* test.

Results

Generation of mAb against mouse EphB4. To investigate EphB4 expression at the protein level in tumor cells, we generated antimouse EphB4 mAb (clone VEB4-7E4) and first observed EphB4 expression in the BaF3 hematopoietic cell line induced with ectopic EphB4 (BaF3/EphB4, Fig. 1*A*) by flow cytometric analysis (Fig. 1*B*) and Western blotting (Fig. 1*C*). As observed in Fig. 1*B*, this mAb recognized EphB4 on BaF3 cells and this reaction to EphB4 by the mAb was almost completely suppressed by soluble EphB4 protein, suggesting that this reaction was specific to EphB4. Moreover, this mAb could recognize a 120-kDa protein from BaF3/EphB4 cell lysates but not from BaF3/mock cells (Fig. 1*C*). In immunohistochemical staining of hind limb muscle using LacZ reporter strain to detect expression of ephrinB2 (arteries; ref. 4), together with antibody to CD31/PECAM-1, a pan-endothelial marker, this mAb against EphB4 (VEB4-7E4) did not recognize CD31$^+$ephrinB2$^+$ arterial ECs but was able to mark CD31$^+$ephrinB2$^-$ ECs (Fig. 1*D*). These reciprocal expression profiles indicated that this mAb could

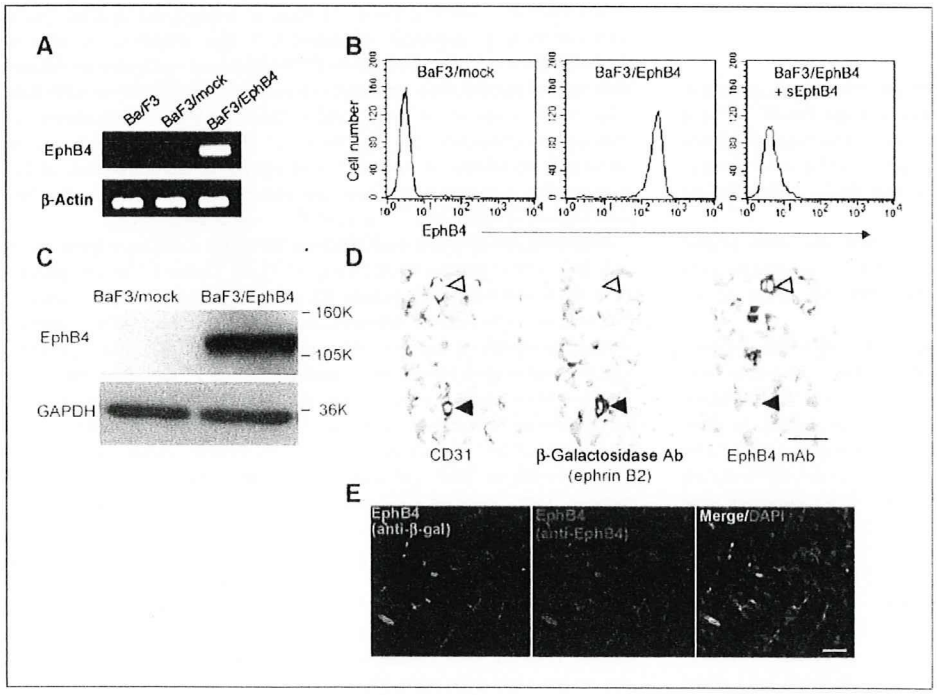

Figure 1. Specificity of generated EphB4 mAb. *A*, RT-PCR analysis of *EphB4* mRNA in BaF3 cells, BaF3 cells transfected with mock (BaF3/mock), or *EphB4* (BaF3/EphB4) plasmid. *B*, FACS analysis of EphB4 expression in BaF3/mock and BaF3/EphB4 cells. Soluble EphB4-FC chimeric protein (sEphB4) was used for analyzing specific binding of EphB4 mAb to EphB4. *C*, Western blotting analysis for detecting EphB4 protein from cell lysates of BaF3/mock or BaF3/EphB4 with EphB4 mAb and anti-GAPDH antibody. *D*, serial sections from mouse hind limb muscle of 8-week-old ephrinB2$^{LacZ/+}$ mice were stained with anti-CD31, anti–β-galactosidase, or anti-EphB4 antibodies. *Open* and *closed arrows*, CD31$^+$ephrinB2$^-$EphB4$^+$ and CD31$^+$ephrinB2$^+$EphB4$^-$ blood vessels, respectively. *Bar*, 40 μm. *E*, sections from mouse hind limb muscle of 8-week-old EphB4$^{LacZ/+}$ mice were stained with anti–β-galactosidase and anti-EphB4 antibodies. Nuclei were stained with DAPI. *Bar*, 40 μm.

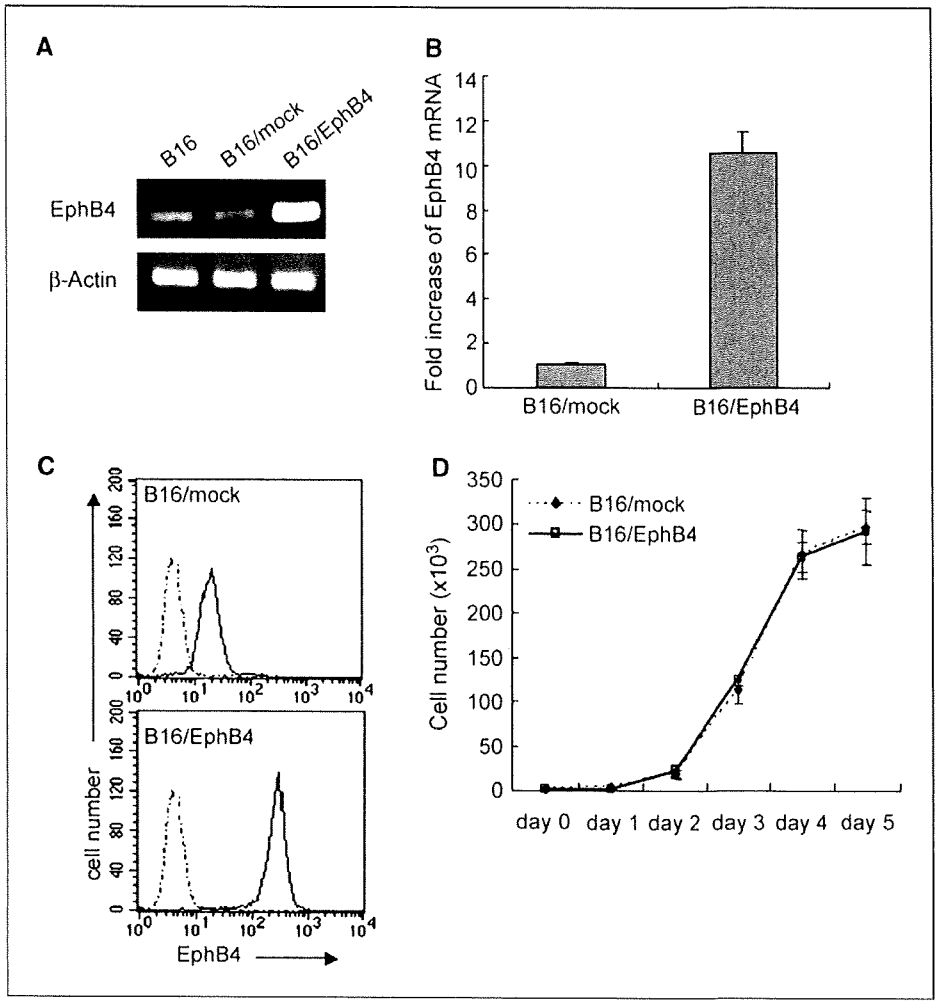

Figure 2. Effect of EphB4 overexpression in B16 cells on *in vitro* proliferation. B16 cells were transfected with mock (B16/mock) or *EphB4* (B16/EphB4) expression vectors. *A*, RT-PCR analysis of *EphB4* mRNA expression in B16, B16/mock, or B16/EphB4 cells. *B*, real-time PCR analysis of *EphB4* mRNA in B16/mock or B16/EphB4 cells. *C*, FACS analysis of *EphB4* protein expression by EphB4 mAb in B16/mock or B16/EphB4 cells. *Dashed line*, intensity of negative control. *D*, *in vitro* proliferation analysis.

react with EphB4. Moreover, to detect the expression of EphB4 in hind limb muscle from LacZ reporter mice (2), β-galactosidase–positive ECs were exclusively stained with anti-EphB4 antibody (Fig. 1*E*). Taken together, we concluded that this mAb (VEB4-7E4) reacts specifically with EphB4.

EphB4 overexpression did not alter *in vitro* proliferation of B16 melanoma cells. We looked for a tumor cell line that endogenously expresses EphB4 but not ephrinB2. Among several mouse and human tumor cell lines tested, we found that B16 mouse melanoma cells matched these criteria (Supplementary Table S1). Therefore, using B16 melanoma cells, we first observed whether overexpression of EphB4 in B16 cells affects cell growth. Overexpression of EphB4 stably transduced in B16 cells (B16/EphB4) was compared with that in control B16 cells transduced with mock vector (B16/mock) by RT-PCR (Fig. 2*A*) and real-time PCR (Fig. 2*B*) analyses at the mRNA level. Overexpression of EphB4 in B16/EphB4 cells was also confirmed by FACS analysis at the protein level (Fig. 2*C*). An *in vitro* proliferation of B16/EphB4 and B16/mock cells was observed. Results indicated that B16 overexpression did not alter the growth of B16 cells (Fig. 2*D*). We cloned several EphB4-overexpressing B16 cells and there was no difference from the results obtained with the subclones (data not shown).

EphB4 overexpression suppressed tumor growth in *in vivo* xenograft assay. To investigate the function of EphB4 in B16 cells *in vivo*, B16/EphB4 and B16/mock cells were injected s.c. into C57BL/6 mice. To observe tumor growth, the tumor size was measured every 3 days. Eighteen days after inoculation of tumor cells, the tumors were removed from the mice and the tumor mass was weighed. Although EphB4 overexpression did not affect the *in vitro* growth of B16 cells (see above), the *in vivo* growth of B16/EphB4 cells was clearly inhibited in comparison with that of B16/mock cells (Fig. 3*A*).

Although EphB4 protein expression level in parental B16 cells was low (Fig. 2*C*), to confirm dose dependency of EphB4 in tumor growth, we knocked down the *EphB4* gene in B16 cells and then studied *in vitro* and *in vivo* growth. As shown in Fig. 3*B*, on transfection with plasmids containing shRNA oligonucleotides that specifically recognized *EphB4* sequences, *EphB4* expression of B16 cells (B16/shRNA) was reduced compared with the level of expression when the cells were transfected with a plasmid containing nonspecific shRNA (B16/scr). *In vitro* cell proliferation was not affected by the depletion of EphB4 from B16 cells (Fig. 3*B*, *middle*); however, we confirmed that, *in vivo*, EphB4 depletion in B16 cells enhanced tumor growth (Fig. 3*B*, *right*). These results clearly indicated that reduction of EphB4 expression accelerates tumor growth in B16 cells.

EphB4 overexpression in B16 cells inhibits formation of blood vessels with an arterial phenotype in tumors. To clarify the

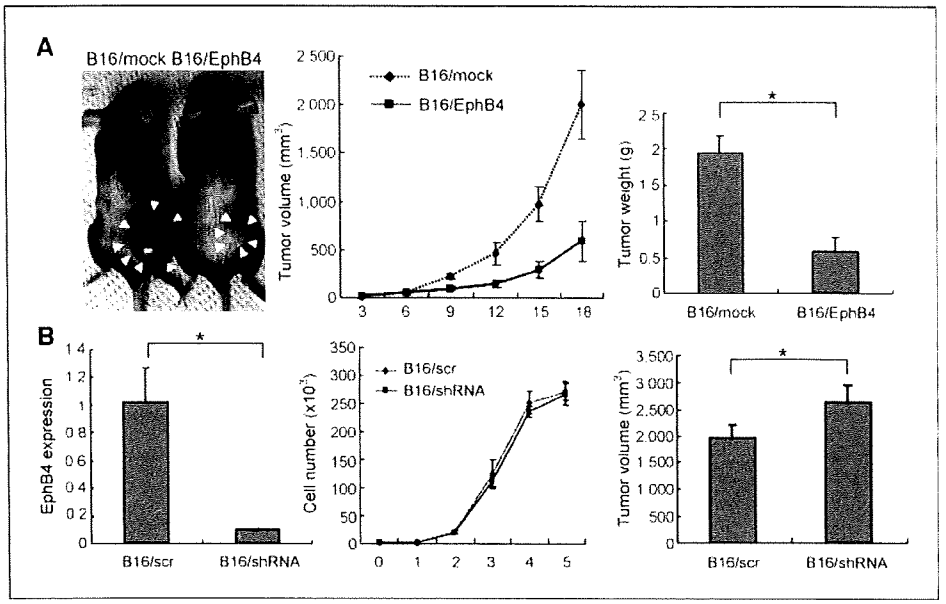

Figure 3. Tumor growth in inverse proportion to the expression levels of EphB4. *A, left,* gross appearance of tumors derived from B16/mock or B16/EphB4 cells on day 18 after tumor cell inoculation. *Arrows,* tumor area. *Middle,* tumor volume measured every 3 d after tumor cell inoculation. *Right,* tumor weight on day 18 after tumor cell inoculation. *, $P < 0.05$ ($n = 5$). *B, left,* real-time RT-PCR analysis of *EphB4* mRNA expression in B16 cells transduced by an *EphB4*-specific shRNA (B16/shRNA) or a nonspecific insert (B16/scr). *, $P < 0.05$ ($n = 3$). *Middle, in vitro* proliferation analysis. *Right,* tumor volume was determined on day 18 after s.c. inoculation of B16/shRNA or B16/scr cells into C57BL/6 mice. *, $P < 0.05$ ($n = 5$).

suppressive effect on tumor growth of EphB4 overexpression in B16 cells, we stained tumor tissues with anti-CD31 antibody and found that the number of blood vessels in tumors from B16/EphB4 cells was almost half that found in tumors from B16/mock cells (Fig. 4*A* and *B*). On the other hand, the difference in vessel density between B16/mock and B16/shEphB4 was not large compared with that between B16/mock and B16/EphB4; however, vessel density was slightly, but statistically significantly, higher in the B16/shEphB4 tumor than in the control B16/mock tumor (Fig. 4*A* and *B*).

These results suggested that EphB4 overexpression in B16 cells suppressed tumor angiogenesis.

Nevertheless, the method by which EphB4 affects blood vessel development was not clear. To investigate the properties of blood vessels in tumors, we inoculated B16/EphB4 and B16/mock cells s.c. into LacZ reporter mice to detect the expression of ephrinB2 (4) or EphB4 (2), together with anti-CD31 antibody, in tumor sections. As shown in Fig. 5, in tumors derived from B16/mock cells, nearly half of the ECs were ephrinB2$^+$ and had an arterial phenotype. On

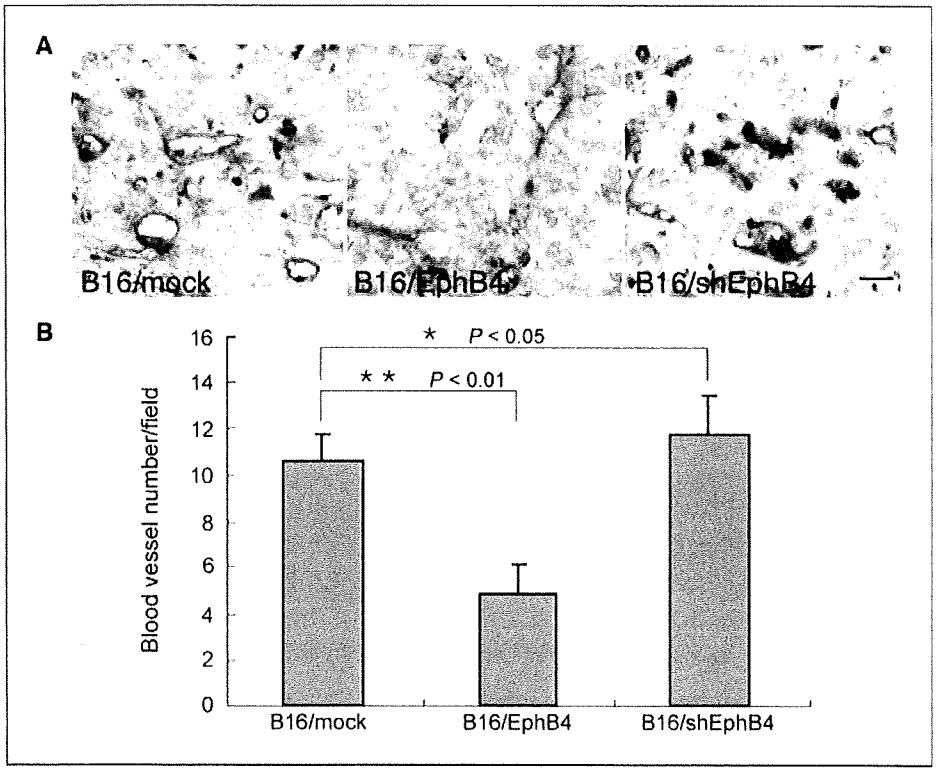

Figure 4. Effect of EphB4 overexpression in B16 cells on tumor angiogenesis. *A,* blood vessel formation in tumors derived from B16/mock (*left*), B16/EphB4 (*middle*), or B16/shEphB4 (*right*) cells. Sections were obtained from the tumors on day 18 after inoculation with the respective tumor cells and stained with anti-CD31 mAb (*red*). *Bar,* 40 μm. *B,* quantitative evaluation of blood vessels from 30 random fields of three independent tumors, as indicated. *, $P < 0.05$; **, $P < 0.01$.

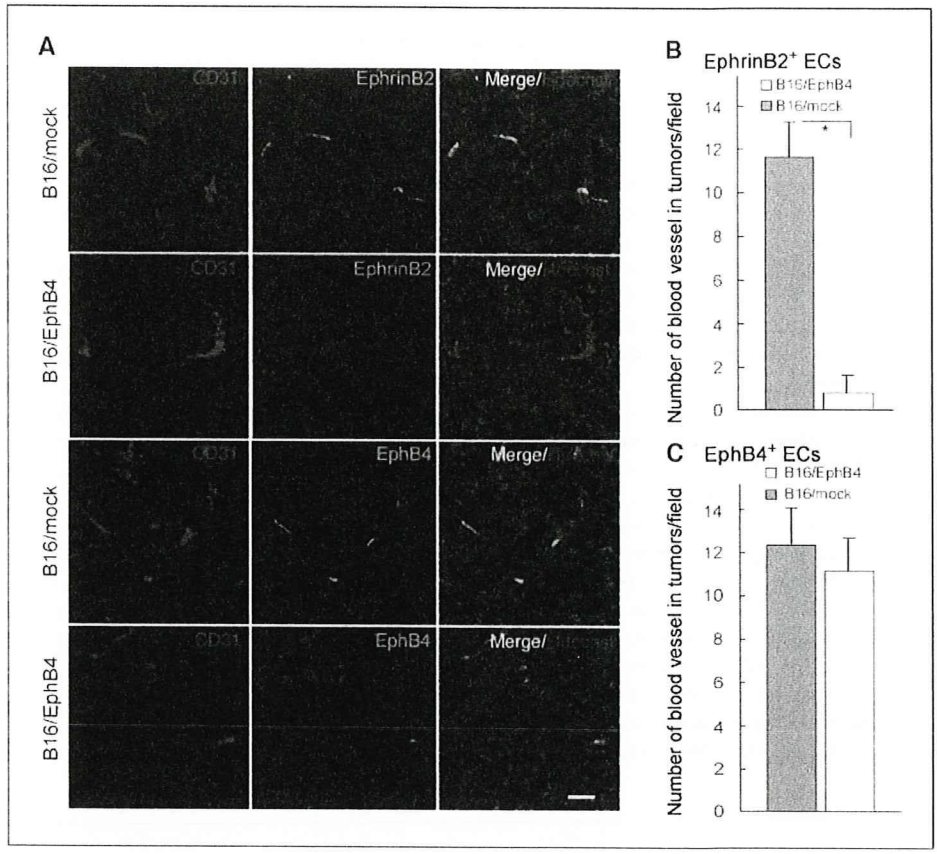

Figure 5. Effect of EphB4 overexpression in B16 cells on the arterial-venous patterning in tumors. *A*, sections derived from tumors generated by s.c. inoculation of B16/mock (*top lane*) or B16/EphB4 (*second lane*) into ephrinB2$^{LacZ/+}$ mice for 18 d were doubly stained with anti-CD31 (*red*) and anti–β-galactosidase (*green*) antibodies. Merged image with CD31 and β-galactosidase staining was shown as indicated. Nuclei were counterstained with Hoechst. Sections derived from tumors generated by s.c. inoculation of B16/mock (*third lane*) or B16/EphB4 (*bottom lane*) into EphB4$^{LacZ/+}$ mice after 18 d were doubly stained with anti-CD31 (*red*) and anti–β-galactosidase (*green*) antibodies. Merged image with CD31 and β-galactosidase staining was shown as indicated. Nuclei were counterstained with Hoechst. *Bar*, 40 μm. *B* and *C*, quantitative evaluation of ephrinB2$^+$ arteries (*B*) or EphB4$^+$ veins (*C*) from 30 random fields of three independent tumors, as indicated. *, $P < 0.05$.

the other hand, in B16/EphB4 tumors, ephrinB2$^+$ ECs were difficult to detect; only ~6% of ECs in these tumors expressed ephrinB2. By contrast, EphB4$^+$ ECs having a venous phenotype were observed in equal numbers in tumors derived from both B16/mock and B16/EphB4 cells. Therefore, we concluded that EphB4 in B16 cells selectively suppressed the formation of blood vessels with an arterial phenotype.

EphB4 in B16 cells induces apoptosis of ephrinB2$^+$ ECs. Because EphB4 suppressed the appearance of ephrinB2$^+$ ECs in tumors, the final aspect we investigated was how EphB4 overexpression in B16 cells might be affecting ephrinB2$^+$ cells *in vitro*. To achieve this, we induced ephrinB2 into the murine SVEC EC line and generated stably and strongly ephrinB2-expressing ECs (SVEC/ephrinB2), because endogenous ephrinB2 expression was weak in the original SVECs (Supplementary Fig. S1), and cocultured these cells with B16/mock or B16/EphB4 cells (Fig. 6). After coculturing for 24 h, apoptosis of SVEC/ephrinB2 in B16/mock cells or B16/EphB4 cells, B16/mock cells cocultured with SVEC/ephrinB2, and B16/EphB4 cells cocultured with SVEC/ephrinB2 cells was observed by staining with Annexin V and nuclear dye DAPI (Fig. 6*A* and *B*). Results showed that B16/EphB4 cells enhanced apoptosis (Annexin V$^+$DAPI$^-$) and cell death (Annexin V$^+$DAPI$^+$) in SVEC/ephrinB2 cells compared with B16/mock cells (Fig. 6*A* and *B*). When compared with cell death of SVEC/ephrinB2 in B16/mock cells, similar apoptosis and cell death of SVEC/ephrinB2 cells in normal culture conditions (i.e., SVEC/ephrinB2 cells not cocultured with B16 cells) was observed (data not shown). The apoptotic effect of B16/EphB4 cells on SVEC/ephrinB2 cells in this coculturing system was suppressed by the separation of the two cell types by means of a 0.4-μm-pore filter (Fig. 6*A* and *B*). Moreover, blockade of interactions between SVEC/ephrinB2 and B16/EphB4 cells with soluble EphB4 proteins abolished the B16/EphB4-mediated increase in cell death of SVEC/ephrinB2 (Fig. 6*A* and *B*). Therefore, we concluded that apoptosis of SVEC/ephrinB2 cells was accelerated by cell-to-cell contact with B16/EphB4 cells.

On the other hand, in the case of B16 cells, the percentage (Fig. 6*A* and *B*) and absolute cell number (data not shown) of apoptotic and dead cells from B16/EphB4 cells cocultured with SVEC/ephrinB2 cells were not statistically significantly different compared with those from B16/mock cells cocultured with SVEC/ephrinB2 cells. Moreover, such apoptosis and cell death was also observed in B16/mock and B16/EphB4 under normal culture conditions without coculturing with SVEC/ephrinB2 cells (data not shown). This suggested that ephrinB2 does not affect EphB4 in B16 cells, in terms of cell viability, as a forward signaling.

Taken together, we concluded that EphB4 overexpression in B16 melanoma cells induces cell apoptosis of ephrinB2$^+$ ECs. Therefore, when inoculated into mice, B16/EphB4 cells might suppress the survival of ephrinB2$^+$ ECs, resulting in insufficient arterial-venous blood vessel distribution and the inhibition of tumor growth.

Discussion

Although the EphB4 receptor has been reported to be expressed in various tumor cells (14–19), its exact function in arterio-venous specification has not yet been elucidated. In this study, we showed

that EphB4 overexpression in B16 melanoma cells suppressed tumor angiogenesis, especially the development of ephrinB2$^+$ ECs with an arterial phenotype in tumors. By coculturing ephrinB2-expressing ECs (SVEC induced with ephrinB2) with EphB4-overexpressing B16 cells, we found that EphB4 reverse signaling via ephrinB2 was involved in the apoptosis of ephrinB2$^+$ ECs. Ideally, it was better to coculture ephrinB2$^+$ ECs in tumors derived from B16 cells with B16/EphB4 cells to examine the nature of the arterial ECs affected by EphB4 in tumor cells. However, due to technical problems, we experienced difficulties in culturing primary ECs from tumors *in vitro*. Moreover, there was no antibody available to isolate ephrinB2$^+$ ECs from tumors using a cell sorter. Therefore, we used SVEC, an EC line, stably and strongly induced with ephrinB2.

Thus far, a variety of functions of Eph receptors and their ephrin ligands have been reported in the areas of cell migration, repulsion, and adhesion (5, 6, 8, 31, 32). Although it has been proposed that this receptor/ligand system is not involved in cell proliferation, nevertheless, it has also been reported that ephrin-A/EphA receptor signaling plays a key role in controlling the size of the mouse cerebral cortex by regulating cortical progenitor cell apoptosis (33). Moreover, we previously reported that EphB4 reverse signaling via ephrinB2 inhibited the mitotic activity of ephrinB2$^+$ ECs (25). Because of bidirectional signals termed forward signaling via EphB4 and reverse signaling via ephrinB2, we suggested that EphB4/ephrinB2 works on the arterial-venous interface through this bidirectional repulsion to form the arterial-venous boundary. However, in this report, we have clearly shown that reverse signaling via ephrinB2 led to the apoptosis of ephrinB2$^+$ cells (SVEC/ephrinB2), whereas forward signaling via EphB4 in tumor cells did not induce the apoptosis of EphB4$^+$ tumor cells (B16/EphB4). Taken together, this suggested that reverse signaling via ephrinB2 in ECs might terminate arteriogenesis during angiogenesis or induce regression of newly developed arterial blood vessels.

The function of EphB4/ephrinB2 in the development of blood vessel formation during embryogenesis has been the focus of research (2–4). In addition, its role in tumor angiogenesis has also been examined by a variety of methods, such as systemic or local administration of soluble EphB4 receptors (34, 35), site-specific expression of EphB4 or kinase-dead EphB4 in ECs retrovirally (36), and a xenograft model using breast cancer cells expressing kinase-dead EphB4 receptor (37). In the case of soluble EphB4 administration, tumor angiogenesis was perturbed (34, 35). This effect might result from the suppression of forward and reverse signaling via EphB4 and ephrinB2, respectively. Recently, the enhancement of EphB4 reverse signaling via ephrinB2 in ECs, in which EphB4 was ectopically induced in the ECs of tumors, has been reported to increase vascular density and permeability of blood vessels in tumors (36). These results indicated that EphB4/ephrinB2 signaling is active in tumor angiogenesis. However, the function of EphB4 in tumor cells for blood vessel formation has not been well clarified. One piece of research has shown that kinase-dead EphB4 expressed in tumor

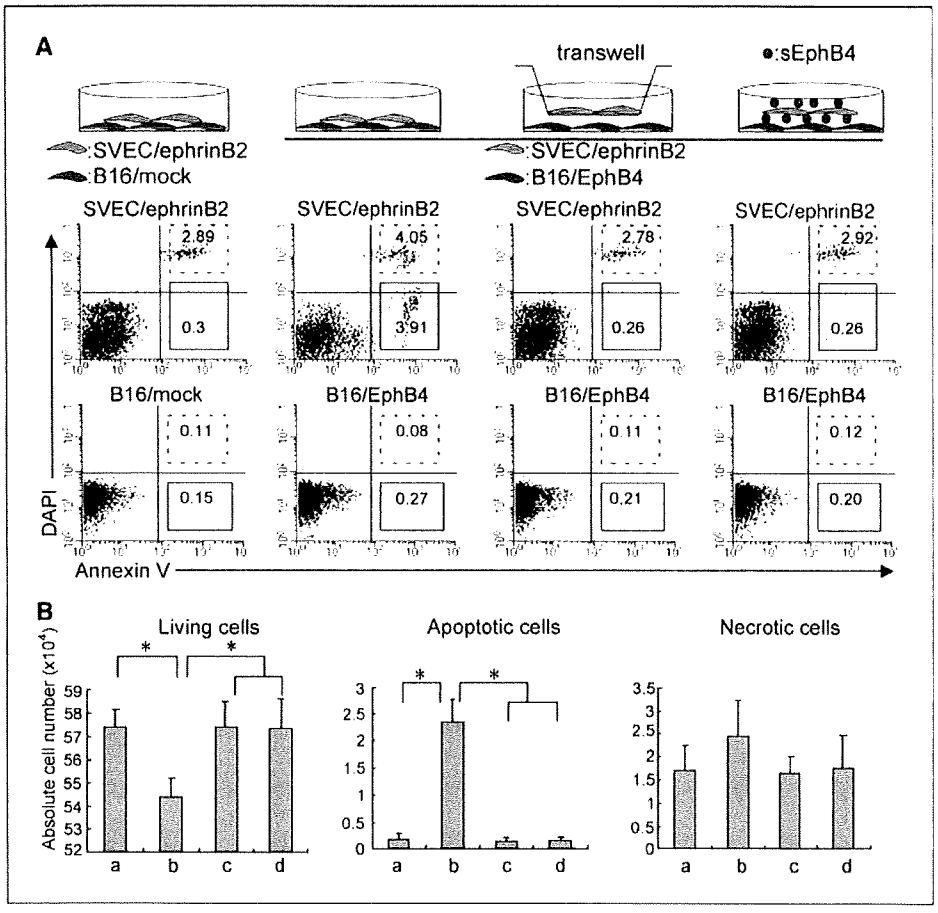

Figure 6. Effect of EphB4 overexpression in B16 cells on ephrinB2$^+$ SVECs as a reverse signaling via ephrinB2. *A, first* and *second columns,* direct coculture of SVEC/ephrinB2 cells with B16/mock or B16/EphB4 cells, respectively. *Third column,* indirect coculture of SVEC/ephrinB2 cells with B16/EphB4 cells separated with a transmembrane having 0.4-μm pores. *Fourth column,* direct coculture of SVEC/ephrinB2 cells with B16/EphB4 cells in the presence of soluble EphB4 (sEphB4). Schematic presentation of coculturing is presented on the top. B16 tumor cells or SVECs were prelabeled with PKH26 red fluorescence or PKH67 green fluorescence, respectively. After 24 h of coculture, cells gated by PKH67 or PKH26 discrimination (Supplementary Fig. S2) were analyzed by staining with anti-Annexin V-Cy5 and DAPI by FACS. Numbers in each quadrant indicate the percentage of Annexin V$^+$DAPI$^-$ apoptotic cells (*solid squares*) or Annexin V$^+$DAPI$^+$ dead cells (*dashed squares*) among the total cells. *B,* absolute number of living, apoptotic, or necrotic SVEC/ephrinB2 cells among the number of harvested whole cells in each culture condition as in *A*. *a* to *d,* culture conditions described in *A*: *a,* left; *b,* second; *c,* third; *d,* right. *, $P < 0.05$ ($n = 3$).

cells, in which only reverse signaling via ephrinB2 was enhanced, increased tumor angiogenesis and tumor growth (37). At first glance, there seems to be a discrepancy between these data and those presented here. However, in our experiment, wild-type EphB4 overexpression in B16 tumor cells, in which both forward signaling via EphB4 for tumor cells and reverse signaling via ephrinB2 for ECs cells were enhanced, suppressed the development of ephrinB2$^+$ blood vessels and resulted in the retardation of tumor growth. Therefore, this suggests that secondary inside-out signaling molecules from EphB4$^+$ tumor cells, through forward signaling via EphB4, may induce apoptosis of ephrinB2$^+$ cells with reverse signaling. Recently, it was reported in humans that EphB4 was expressed in human colonic crypts and in early colorectal cancer lesions and that EphB4 expression was lost in advanced colorectal tumors (15). This examination correlates with our data and suggests that, within tumors, the expression of EphB4 inhibits arteriogenesis whereas the loss of EphB4 permits the supply of oxygen and nutrients by establishing arterial-venous circulation.

Recently, it was reported that the expression level of EphB4 in human ovarian cancers is correlated with poor response to chemotherapy (19). Our results can offer two possible, complementary, explanations for this finding. From our study, it seems that EphB4 overexpression in tumor cells inhibits the organization of arterio-venous patterning in tumors, which could increase the difficulty anticancer drugs have in penetrating deep into tumor tissue, whereas, additionally, this overexpression has an inhibitory effect on rapid tumor growth. It is well known that blood vessels in tumors are disorganized compared with those observed in normal tissue, and permeability is relatively suppressed in the tumor environment. Recently, a new therapeutic concept has emerged whereby the artificially induced normalization of blood vessels in tumors could allow the penetration of anticancer drugs deep into the site of the tumors (38); normalization of arterial-venous patterning might be one such strategy for cancer therapy. In this study, we used a B16 mouse melanoma cell line to observe the function of EphB4 in ephrinB2$^+$ EC development precisely because of the lack of ephrinB2 expression in B16 cells. In humans, there are no published reports showing EphB4 expression in primary melanomas but several articles have indicated that most human melanoma cell lines express EphB4 (14, 39). However, although coexpression of EphB4/ephrinB2 in human melanoma tissue samples or melanoma cell lines has not been reported, in both settings the expression level of ephrinB2 has been reported to vary, and it has been proposed that expression level correlates with malignancy (14, 40). The functions of ephrinB2 and EphB4 in melanomas seem to be redundant for tumorigenesis in which ephrinB2 and EphB4 are associated with both tumor cell viability and generation of microenvironment. To further clarify the function of the EphB4/ephrinB2 system, it will be necessary to examine how EphB4 and ephrinB2 expression in tumor cells is regulated during the ontogeny of tumors.

Acknowledgments

Received 2/7/2007; revised 6/15/2007; accepted 7/29/2007.

Grant support: Grant-in-Aid from The Ministry of Education, Culture, Sports, Science, and Technology of Japan (N. Takakura).

The costs of publication of this article were defrayed in part by the payment of page charges. This article must therefore be hereby marked *advertisement* in accordance with 18 U.S.C. Section 1734 solely to indicate this fact.

We thank N. Fujimoto for preparation of plasmid DNA and K. Fukuhara for administrative assistance.

References

1. Risau W. Mechanisms of angiogenesis. Nature 1997; 386:671–4.
2. Wang HU, Chen ZF, Anderson DJ. Molecular distinction and angiogenic interaction between embryonic arteries and veins revealed by ephrinB2 and its receptor EphB4. Cell 1998;93:741–53.
3. Adams RH, Wilkinson GA, Weiss C, et al. Roles of ephrinB ligands and EphB receptors in cardiovascular development: demarcation of arterial/venous domains, vascular morphogenesis, and sprouting angiogenesis. Genes Dev 1999;13:295–306.
4. Gerety SS, Wang HU, Chen ZF, Anderson DJ. Symmetrical mutant phenotypes of the receptor EphB4 and its specific transmembrane ligand ephrin-B2 in cardiovascular development. Mol Cell 1999;4:403–14.
5. Kullander K, Klein R. Mechanisms and functions of Eph and ephrin signaling. Nat Rev Mol Cell Biol 2002;3: 475–86.
6. Mellitzer G, Xu Q, Wilkinson DG. Control of cell behaviour by signalling through Eph receptors and ephrins. Curr Opin Neurobiol 2000;10:400–8.
7. Gale NW, Baluk P, Pan L, et al. Ephrin-B2 selectively marks arterial vessels and neovascularization sites in the adult, with expression in both endothelial and smooth-muscle cells. Dev Biol 2001;230:151–60.
8. Wilkinson DG. Multiple roles of EPH receptors and ephrins in neural development. Nat Rev Neurosci 2001;2: 155–64.
9. Knoll B, Drescher U. Ephrin-As as receptors in topographic projections. Trends Neurosci 2002;25:145–9.
10. Barrios A, Poole RJ, Durbin L, Brennan C, Holder N, Wilson SW. Eph/Ephrin signaling regulates the mesenchymal-to-epithelial transition of the paraxial mesoderm during somite morphogenesis. Curr Biol 2003;13: 1571–82.
11. Adams RH. Vascular patterning by Eph receptor tyrosine kinases and ephrins. Semin Cell Dev Biol 2002; 13:55–60.
12. Adams RH, Klein R. Eph receptors and ephrin ligands: essential mediators of vascular development. Trends Cardiovasc Med 2000;10:183–8.
13. Adams RH, Diella F, Hennig S, Helmbacher F, Deutsch U, Klein R. The cytoplasmic domain of the ligand ephrinB2 is required for vascular morphogenesis but not cranial neural crest migration. Cell 2001;104: 57–69.
14. Nakamoto M, Bergemann AD. Diverse roles for the Eph family of receptor tyrosine kinases in carcinogenesis. Microsc Res Tech 2002;59:58–67.
15. Batlle E, Bacani J, Begthel H, et al. EphB receptor activity suppresses colorectal cancer progression. Nature 2005;435:1126–30.
16. Liu W, Ahmad SA, Jung YD, et al. Coexpression of ephrin-Bs and their receptors in colon carcinoma. Cancer 2002;94:934–9.
17. Xia G, Kumar SR, Masood R, et al. Up-regulation of EphB4 in mesothelioma and its biological significance. Clin Cancer Res 2005;11:4305–15.
18. Xia G, Kumar SR, Stein JP, et al. EphB4 receptor tyrosine kinase is expressed in bladder cancer and provides signals for cell survival. Oncogene 2006;25: 769–80.
19. Wu Q, Suo Z, Kristensen GB, Baekelandt M, Nesland JM. The prognostic impact of EphB2/B4 expression on patients with advanced ovarian carcinoma. Gynecol Oncol 2006;102:15–21.
20. Berclaz G, Flutsch B, Altermatt HJ, et al. Loss of EphB4 receptor tyrosine kinase protein expression during carcinogenesis of the human breast. Oncol Rep 2002;9:985–9.
21. Masood R, Kumar SR, Sinha UK, et al. EphB4 provides survival advantage to squamous cell carcinoma of the head and neck. Int J Cancer 2006;119:1236–48.
22. Berclaz G, Karamitopoulou E, Mazzucchelli L, et al. Activation of the receptor protein tyrosine kinase EphB4 in endometrial hyperplasia and endometrial carcinoma. Ann Oncol 2003;14:220–6.
23. Takai N, Miyazaki T, Fujisawa K, Nasu K, Miyakawa I. Expression of receptor tyrosine kinase EphB4 and its ligand ephrin-B2 is associated with malignant potential in endometrial cancer. Oncol Rep 2001;8:567–73.
24. Tang XX, Brodeur GM, Campling BG, Ikegaki N. Coexpression of transcripts encoding EPHB receptor protein tyrosine kinases and their ephrin-B ligands in human small cell lung carcinoma. Clin Cancer Res 1999; 5:455–60.
25. Sorokin L, Girg W, Gopfert T, Hallmann R, Deutzmann R. Expression of novel 400-kDa laminin chains by mouse and bovine endothelial cells. Eur J Biochem 1994;223:603–10.
26. Zhang XQ, Takakura N, Oike Y, et al. Stromal cells expressing ephrin-B2 promote the growth and sprouting of ephrin-B2(+) endothelial cells. Blood 2001;98: 1028–37.
27. Takakura N, Yoshida H, Ogura Y, Kataoka H, Nishikawa S, Nishikawa S. PDGFRα expression during mouse embryogenesis: immunolocalization analyzed by whole-mount immunohistostaining using the monoclonal anti-mouse PDGFRα antibody APA5. J Histochem Cytochem 1997;45:883–93.
28. Takakura N, Watanabe T, Suenobu S, et al. A role for hematopoietic stem cells in promoting angiogenesis. Cell 2000;102:199–209.

29. Takakura N, Huang XL, Naruse T, et al. Critical role of the TIE2 endothelial cell receptor in the development of definitive hematopoiesis. Immunity 1998;9: 677–86.
30. Okamoto R, Ueno M, Yamada Y, et al. Hematopoietic cells regulate the angiogenic switch during tumorigenesis. Blood 2005;105:2757–63.
31. Holmberg J, Clarke DL, Frisen J. Regulation of repulsion versus adhesion by different splice forms of an Eph receptor. Nature 2000;408:203–6.
32. Cowan CA, Henkemeyer M. Ephrins in reverse, park and drive. Trends Cell Biol 2002;12:339–46.
33. Depaepe V, Suarez-Gonzalez N, Dufour A, et al. Ephrin signalling controls brain size by regulating apoptosis of neural progenitors. Nature 2005;435: 1244–50.
34. Kertesz N, Krasnoperov V, Reddy R, et al. The soluble extracellular domain of EphB4 (sEphB4) antagonizes EphB4-2 interaction, modulates angiogenesis, and inhibits tumor growth. Blood 2006;107:2330–8.
35. Martiny-Baron G, Korff T, Schaffner F, et al. Inhibition of tumor growth and angiogenesis by soluble EphB4. Neoplasia 2004;6:248–57.
36. Erber R, Eichelsbacher U, Powajbo V, et al. EphB4 controls blood vascular morphogenesis during postnatal angiogenesis. EMBO J 2006;25:628–41.
37. Noren NK, Lu M, Freeman AL, Koolpe M, Pasquale EB. Interplay between EphB4 on tumor cells and vascular ephrin-B2 regulates tumor growth. Proc Natl Acad Sci U S A 2004;101:5583–8.
38. Jain RK. Normalization of tumor vasculature: an emerging concept in antiangiogenic therapy. Science 2005;307:58–62.
39. Bennett BD, Wang Z, Kuang WJ, et al. Cloning and characterization of HTK, a novel transmembrane tyrosine kinase of the EPH subfamily. J Biol Chem 1994;269: 14211–8.
40. Vogt T, Stolz W, Welsh J, et al. Overexpression of Lerk-5/Eplg5 messenger RNA: a novel marker for increased tumorigenicity and metastatic potential in human malignant melanomas. Clin Cancer Res 1998;4: 791–7.

STEM CELLS
TISSUE-SPECIFIC STEM CELLS

Cardiac Stem Cells in Brown Adipose Tissue Express CD133 and Induce Bone Marrow Nonhematopoietic Cells to Differentiate into Cardiomyocytes

YOSHIHIRO YAMADA,[a,b,c] SHIN-ICHIRO YOKOYAMA,[d] XIANG-DI WANG,[b] NOBORU FUKUDA,[d] NOBUYUKI TAKAKURA[a,b,c]

[a]Department of Signal Transduction, Research Institute for Microbial Diseases, Osaka University, Osaka, Japan; [b]Department of Stem Cell Biology, Cancer Research Institute of Kanazawa University, Kanazawa, Japan; [c]PREST, Japan Science and Technology Agency, Saitama, Japan; [d]Second Department of Internal Medicine, Nihon University School of Medicine, Tokyo, Japan

Key Words. AC133 • Adult bone marrow • Myogenesis • Adipogenesis

ABSTRACT

Recently, there has been noteworthy progress in the field of cardiac regeneration therapy. We previously reported that brown adipose tissue (BAT) contained cardiac progenitor cells that were relevant to the regeneration of damaged myocardium. In this study, we found that CD133-positive, but not c-Kit- or Sca-1-positive, cells in BAT differentiated into cardiomyocytes (CMs) with a high frequency. Moreover, we found that $CD133^+$ brown adipose tissue-derived cells (BATDCs) effectively induced bone marrow cells (BMCs) into CMs. BMCs are considered to have the greatest potential as a source of CMs, and two sorts of stem cell populations, the MSCs and hematopoietic stem cells (HSCs), have been reported to differentiate into CMs; however, it has not been determined which population is a better source of CMs. Here we show that CD133-positive BATDCs induce BMCs into CMs, not through cell fusion but through bivalent cation-mediated cell-to-cell contact when cocultured. Moreover, BMCs induced by BATDCs are able to act as CM repletion in an in vivo infarction model. Finally, we found that $CD45^-CD31^-$ $CD105^+$ nonhematopoietic cells, when cocultured with BATDCs, generated more than 20 times the number of CMs compared with $lin^-c\text{-}Kit^+$ HSCs. Taken together, these data suggest that CD133-positive BATDCs are a useful tool as CM inducers, as well as a source of CMs, and that the nonhematopoietic fraction in bone marrow is also a major source of CMs. STEM CELLS *2007;25:1326–1333*

Disclosure of potential conflicts of interest is found at the end of this article.

INTRODUCTION

Cell transplantation and gene transfer are two of the foremost therapies with potential for regenerating damaged cardiomyocytes (CMs) and enabling revascularization. Embryonic stem cells, skeletal myoblasts, and c-kit- or Sca-1-positive cardiac stem cells (CSCs) in heart tissue have all been reported as candidates for the replacement of CMs; however, each is associated with problems, including those involving allergenic, etiologic, and arrhythmic issues.

Bone marrow cells (BMCs) are a well-known source of various kinds of stem cells. BMCs can contribute to the regeneration of various tissues, and their clinical application is easier than that of other candidates. Recent studies have suggested that CMs might also originate from BMCs, which are composed of at least two cell populations. Among these are hematopoietic cells (HCs) [1, 2] and mesenchymal cells [3–5], both of which have been suggested as sources of CMs. Nevertheless, the ability of the former to differentiate into CMs is by no means clear. Several studies have demonstrated that hematopoietic stem cells (HSCs) can induce myogenic repair by their capacity to differentiate into CMs [1, 2]. However, two other studies, which used an in vivo infarction model, reported that HSCs were incapable of differentiating into CMs [6, 7]. Moreover, Alvarez-Dolado et al. demonstrated that bone marrow (BM)-derived CMs were observed at low frequency and were generated by cell fusion with donor $CD45^+$ HCs [8]. Taken together, the results from these various studies suggest that it remains to be resolved whether plasticity of HSCs truly occurs and which population will prove to be the best source for the repair of damaged cardiac tissue. Moreover, specific molecular cues for the differentiation of CMs from BMCs have not been identified. This lack of knowledge means that, at present, it is difficult to effectively induce immature cells into CMs.

In this study, we show that CD133 is a CSC marker in brown adipose tissue-derived cells (BATDCs), which had been identified previously as a source of CSCs [9]. CD133 was first isolated from neuroepithelial stem cells as mouse Prominin-1 [10]; subsequently, it was reported that $CD34^+$ HSCs isolated from fetal liver, BM, and cord blood expressed CD133 (AC133) [11]. Moreover, CD133 antigen expression was detected in

Correspondence: Nobuyuki Takakura, M.D., Ph.D., Department of Signal Transduction, Research Institute for Microbial Diseases, Osaka University, 3-1 Yamadaoka, Suita-shi, Osaka 565-0871, Japan. Telephone: 81-6-6879-8316; Fax: 81-6-6879-8314; e-mail: ntakaku@biken.osaka-u.ac.jp; Yoshihiro Yamada, M.D., Ph.D., Department of Signal Transduction, Research Institute for Microbial Diseases, Osaka University, 3-1 Yamadaoka, Suita-shi, Osaka 565-0871, Japan. Telephone: 81-6-6879-8316; Fax: 81-6-6879-8314; e-mail: yamaday@biken.osaka-u.ac.jp Received September 19, 2006; accepted for publication January 30, 2007; first published online in STEM CELLS *EXPRESS* February 8, 2007. ©AlphaMed Press 1066-5099/2007/$30.00/0 doi: 10.1634/stemcells.2006-0588

undifferentiated cells, including endothelial progenitor cells [12], fetal brain stem cells [13], embryonic epithelium [14], prostatic epithelial stem cells [15], myogenic cells [16], and certain cancer stem cells, such as retinoblastoma [17] and medulloblastoma [18]. These results indicated that CD133 might be an antigen common to several stem cells, including CSCs, in brown adipose tissue (BAT). Second, we have shown that BMCs could differentiate with high efficiency into CMs by coculturing with BATDCs. In this induction system, we have demonstrated that bivalent cation-mediated cell-to-cell contact was critical for the differentiation of BMCs into CMs, and we have also investigated cadherin-mediated cell contact. Finally, we have demonstrated that in the bone marrow (BM) population, $CD45^-CD31^-CD105^+$ non-HCs could effectively differentiate into CMs, in contrast to the $lin^-c\text{-}Kit^+$ HSCs.

MATERIALS AND METHODS

Cell Preparation and Flow Cytometry

BAT was dissected from the interscapular region of postnatal day 1 (P1) to P7 neonates of C57BL/6 mice. BAT was dissociated by DispaseII (Roche Diagnostics, Mannheim, Germany, http://www.roche-applied-science.com), drawn through a 23-gauge needle, and prepared as a single-cell suspension, as previously reported [9]. BMCs were harvested from femurs and tibias of green fluorescent protein (GFP) transgenic mice (green mice) as previously described [19]. The cell-staining procedure for the flow cytometry was also as previously described [20]. The monoclonal antibodies (mAbs) used in immunofluorescence staining were anti-CD45, -ter119, -CD31, -CD29, -c-kit, -Sca1, -CD105, and -CD133 mAbs (BD Pharmingen, San Diego, http://www.bdbiosciences.com/pharmingen). All mAbs were purified and conjugated with fluorescein isothiocyanate, phycoerythrin (PE), biotin, or allophycocyanin (APC). Biotinylated antibodies were visualized with PE-conjugated streptavidin (BD Pharmingen) or APC-conjugated streptavidin (BD Pharmingen). Cells were incubated for 5 minutes on ice with CD16/32 (FcγIII/II Receptor) (1:100) (Fcblock; BD Pharmingen) prior to staining with primary antibody. Cells were incubated in 5% fetal calf serum (FCS)/phosphate-buffered saline (PBS) (washing buffer) with primary antibody for 30 minutes on ice and washed twice with washing buffer. Secondary antibody was added, and the cells were incubated for 30 minutes on ice. After incubation, cells were washed twice with, and suspended in, the washing buffer for fluorescence-activated cell sorting (FACS) analysis. The stained cells were analyzed and sorted with an EPICS flow cytometer (Beckman Coulter, San Jose, CA, http://www.beckmancoulter.com). The sorted cells were added to 24-well dishes (Nunc, Roskilde, Denmark, http://www.nuncbrand.com), precoated with 0.1% gelatin (Sigma-Aldrich, St. Louis, http://www.sigmaaldrich.com), and cultured in Dulbecco's modified Eagle's medium (DMEM) supplemented with 10% FCS and 10^{-5} M 2-mercaptoethanol at 37°C in a 5% CO_2 incubator.

Immunohistochemistry

Immunohistochemical analyses of tissue sections and culture dishes and the tissue fixation procedure were performed as previously described [9, 20]. The fixed specimens were embedded in Optimum Cutting Temperature (OCT) compound (Sakura Finetechnical, Tokyo, http://www.sakuraus.com) and sectioned at 7 μm. Anti-sarcomeric actin (anti-SA) (clone 5C5; Sigma-Aldrich), anti-GATA-4 (Santa Cruz Biotechnology Inc., Santa Cruz, CA, http://www.scbt.com), -MEF2C (Cell Signaling Technology, Beverly, MA, http://www.cellsignal.com), -connexin43 (Sigma-Aldrich), -atrial natriuretic factor (ANF) (Santa Cruz Biotechnology), and -GFP antibodies (Santa Cruz Biotechnology) for tissue sections, and anti-SA, -cardiac troponin T (Santa Cruz Biotechnology), -cardiac troponin I (clone 13–11; Neomarkers, Fremont, CA, http://www.labvision.com) [21–23], -GATA-4, -MEF2C, and -pan-cadherin (Sigma-Aldrich) antibodies for CM culture dishes were used in this assay. In brief, anti-SA was developed with Alexa Fluor 488-, 546-, or 633-conjugated goat anti-mouse IgM (Molecular Probes Inc., Eugene, OR, http://probes.invitrogen.com); anti-pan-cadherin was developed with 546-conjugated goat anti-mouse IgG (Molecular Probes); and anti-cardiac troponin T, cardiac troponin I, -MEF2C, -GATA-4, -connexin43, and -ANF antibodies were developed with Alexa Fluor 488-, 546-, or 633-conjugated goat anti-rabbit IgG (Molecular Probes). Nuclear staining was performed with 4,6-diamidino-2-phenylindole or TOPRO3 (Molecular Probes). Finally, the sections and dishes were observed using an Olympus IX-70 microscope equipped with UPlanFI 4/0.13 and LCPlanFI 20/0.04 dry objective lenses (Olympus, Tokyo, http://www.olympus-global.com). Images were acquired with a CoolSnap digital camera (Roper Scientific, Tokyo, http://www.roperscientific.com). In all assays, an isotype-matched control Ig was used as a negative control, and it was confirmed that the positive signals were not derived from nonspecific background. Images were processed using Adobe Photoshop 7.0 software (Adobe Systems Inc., San Jose, CA, http://www.abode.com).

Transmission Electron Microscopy

Cells were washed in phosphate buffer and fixed with 2% glutaraldehyde and 1% paraformaldehyde in PBS. Samples were post-fixed with 1% osmium in PBS, rinsed, dehydrated, and embedded in araldite (DAKO, Glostrup, Denmark, http://www.dako.com). Then, samples were cut with a diamond knife and examined under a Jeol 100CX (Tokyo, http://www.jeol.co.jp) electron microscope.

Cell Coculture

BATDCs and BMCs were prepared as described above. In situations where $CD133^-$ BATDCs and BMCs were cocultured in contact conditions, 2×10^4 $CD133^+$ BATDCs were plated per well of a 24-well plate and cultured for 10 days before being fixed with 0.5% paraformaldehyde for 15 minutes at room temperature. Fixed cells were washed extensively, first with PBS and then with DMEM/10% FCS. After washing, 1×10^5 BM mononuclear cells (BMMNCs), 1×10^4 $lin^-c\text{-}Kit^+$ HSCs, or 1×10^4 $CD45^-ter119^-CD31^-CD105^+$ MSCs from GFP mice were cultured with fixed BATDCs, as described above, for 10 days and then stained with anti-SA (Sigma-Aldrich), -GATA-4 (Santa Cruz Biotechnology), -MEF-2C (Cell Signaling Technology), and -GFP (MBL International Corp., Nagoya, Japan, http://www.mblintl.com) antibodies. Under separate conditions, $CD133^+$ BATDCs from ROSA26 mice were cocultured on 0.4-μm cell culture inserts (Becton, Dickinson and Company, San Jose, CA, http://www.bd.com) with BMMNCs from green mice in 0.1% gelatin-coated dishes (Becton Dickinson) for 14 days and then stained with anti-SA (Sigma-Aldrich) and anti-GATA-4 (Santa Cruz Biotechnology).

To analyze the diverse signaling between BATDCs and BM-derived cells, we used an anti-E-cadherin antibody (ECCD-1; Calbiochem, La Jolla, CA, http://www.emdbiosciences.com), E-cadherin-Fc, N-cadherin-Fc, and R-cadherin-Fc (all purchased from R&D Systems Inc., Minneapolis, http://www.rndsystems.com).

Reverse Transcription-Polymerase Chain Reaction Analysis

The RNeasy Mini kit (Qiagen, Hilden, Germany, http://www1.qiagen.com) was used for isolation of total RNA from BAT and BMCs. Total RNA was reverse transcribed using the reverse transcription-polymerase chain reaction (RT-PCR) kit (Clontech, Palo Alto, CA, http://www.clontech.com). The cDNA was amplified using Advantage Polymerase Mix (Clontech) in a GeneAmp PCR system, model 9700 (PerkinElmer Life and Analytical Sciences, Norwalk, CT, http://www.perkinelmer.com), by 40–50 cycles. The sequences of the gene-specific primers for RT-PCR were as follows: 5′-α-myosin heavy chain (MHC), TGTCTGCTCTC-CACCGGGAAAATCT; 3′-α-MHC, CATGGCCAATTCTT-GACTCCCATGA; 5′-β-MHC, AACCCACCCAAGTTCGACA AG ATCG; 3′-β-MHC, CCAACTTTCCTGTTGCCCCAAAA ATG; 5′-α-skeletal actin, GGAGATTGTGCGCGACATC AAAGAG; 3′-α-skeletal actin, CTGGTTCCTCCAATGGGA TATCTTC; 5′-α-cardiac actin, TGTGTTACGTCGCC CTGGATTTTGA; 3′-α-cardiac actin, TTGCTGATCCACATTT

GCTGGAAGG; 5′-myosin light chain (MLC)-2a, AGCAGGCACAACGTGGCTCTTCTAA; 3′-MLC-2a, CCTGGGTCATGAGAAGCTGCTTGAA; 5′-MLC-2v, ATGGCACCTTTGTTTGCCAAGAAGC; 3′-MLC-2v, CCCTCGGGATCAAACACCTTAATG; 5′-GATA4, GAGTGAGTCAATTGTGGGGCCATGT; 3′-GATA4, TGCTGCTAGTGGCA TTGCTGGAGTT; 5′-glyceraldehyde-3-phosphate dehydrogenase (G3PDH), TGAAGGTCGGTGTGAACGGATTTGGC; 3′-G3PDH, CATGTAGGCCATGAG GTCCACCAC; 5′-lacZ, GCGTTACCCAACTTAATCG; 3′-lacZ, TGTGAGCGAGTAACAACC; 5′-GFP, TACGGCAAGCTGACCCTGAA; 3′-GFP, TGTGATCGCGCTTCTCGTTG. Each cycle consisted of denaturation at 94°C for 30 seconds and annealing/extension at 70°C for 4 minutes except lacZ and GFP. For lacZ and GFP, each cycle consisted of denaturation at 94°C for 30 second, annealing at 60°C for 1 minute, and extension 72°C for 1 minute.

Myocardial Infarction and Cell Implantation and Echocardiography

BMCs derived from GFP transgenic Sprague-Dawley rats [24] at 2 months old were cocultured for 5 days with CD133$^+$ BATDCs taken from wild-type Sprague-Dawley rats at 3 days, and then the GFP-positive fraction was sorted using an EPICS flow cytometer and implanted into the heart. Myocardial infarctions (MIs) were induced in female Sprague-Dawley rats at 2 months of age as described previously [9]. After verifying the MIs, 10 rats were injected with 2×10^5 cells each, in five opposite regions bordering the infarct, and then sacrificed after 30 days. At each time interval, sham-operated rats were injected with saline as controls. Under ketamine (Dainippon Pharmaceutical, Osaka, Japan, http://www.ds-pharma.co.jp) anesthesia, echocardiography was performed at 29 days. From M mode tracings, left ventriculus end-diastolic and systolic diameter and wall thickness were obtained, and then the percentage of fractional shortening was calculated. Echocardiographic acquisition and analysis were performed by an echocardiographer blinded to treatment group. Results represent the mean of five separate experiments. Mortality was lower, but not significantly different, in the treated rats, averaging 35% in all groups. Protocols were approved by the institutional review board.

Fluorescence In Situ Hybridization Staining

After staining of CMs with anti-SA antibody as described above, we performed fluorescence in situ hybridization (FISH) to determine the presence of rat X and Y chromosomes (Cambio, Cambridge, U.K., http://www.cambio.co.uk) according to the manufacturer's instructions. A digestion with proteinase K (DAKO) (20 μg/ml at 37°C, 5 minutes) was added at the beginning of the FISH protocol. Nuclear staining was performed with TOPRO3 (Molecular Probes). Pictures were taken by confocal microscope (LSM510; Carl Zeiss MicroImaging, Inc., Göttingen, Germany, http://www.zeiss.com).

RESULTS

Surface Phenotype of CM Progenitors in BAT

A putative stem cell population has recently been identified in adipose tissue [25]. This cell population expressed multiple CD marker antigens, such as CD29, CD44, CD90, and CD105, similar to those observed on MSCs. We previously reported that BATDCs included cells that are able to differentiate into CMs [9], and another group has demonstrated the capacity of adipose tissue-derived mesenchymal cells to differentiate into CMs [26]. Other reports have indicated that cardiac progenitor cells in the adult heart expressed c-Kit and Sca-1, which were first established as HSC markers [21, 27]. Therefore, using flow cytometric analysis, we analyzed several stem cell markers and multiple CD markers on cells from BATDCs, which can differentiate into CMs. First, we checked for ter119 (erythrocyte marker), CD45 (LCA) (panleukocyte marker), and CD31 (endothelial marker). Among CD45$^-$ter119$^-$CD31$^-$ cells (nonhematopoietic, nonendothelial cells), c-Kit, Sca-1, and CD133 expression was observed on 1.4%, 16.6%, and 3.5% of total BATDCs, respectively (Fig. 1A). To clarify which populations have a high potential to produce CMs, we cultured a CD45$^-$ter119$^-$CD31$^-$ subpopulation fractionated by c-Kit, Sca-1, or CD133 expression. Among them, CD133-positive BATDCs differentiated into CMs with a higher incidence compared with cells in other fractions and CD29-positive (CD45$^-$ter119$^-$CD31$^-$) cells, which we had previously reported as a CM-enriched population (Fig. 1C). Indeed, approximately 50% of adherent cells from cultured CD133-positive cells among CD45$^-$ter119$^-$CD31$^-$ cells differentiated into SA$^+$GATA-4$^+$ (Fig. 1B, a and b, 1C, a and b), cardiac-troponin T$^+$GATA-4$^+$ (Fig. 1B, c and d), and cardiac-troponin I$^+$MEF2C$^+$ (Fig. 1B, e and f). Furthermore, electron microscopic analysis indicated that these cells had cellular structures typical of CMs, such as an organized sarcomere with typical cross-strain, developed Z-bands, long mitochondria in the cytoplasm, and centrally positioned nuclei (Fig. 1B, g). To provide additional evidence that CD133$^+$ BATDCs have the phenotype of CMs, we performed pharmacological studies (supplemental online data). The calcium antagonist verapamil slowed the beating rate, and the β-agonist isoproterenol induced a dose-dependent increase of the spontaneous contraction rate; however, the β-adrenergic antagonist propranolol reversed the isoproterenol-induced acceleration. These results also indicated that CD133$^+$ BATDCs have the functional character of CMs.

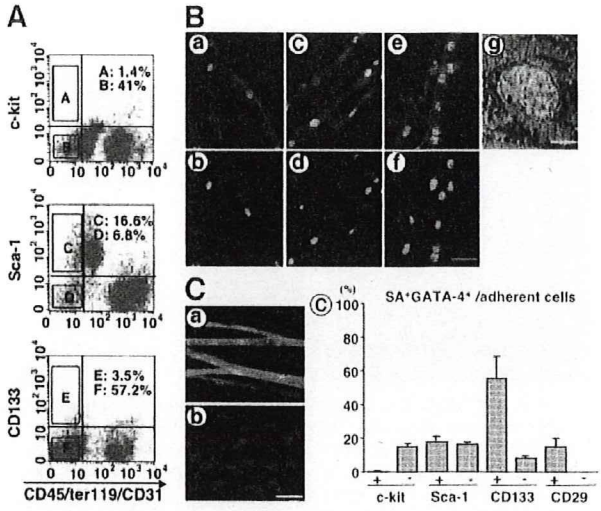

Figure 1. Phenotype of cardiomyocyte (CM) stem cells in brown adipose tissue (BAT). **(A):** Cells derived from BAT were stained with a mixture of anti-CD45, -ter119, and -CD31 antibodies (*x*-axis) and anti-c-Kit, -Sca-1 or -CD133 antibody (*y*-axis). **(B):** Immunocytochemical analysis and transmission electromicrograph of CMs derived from CD133$^+$ (CD45$^-$ter119$^-$CD31$^-$) BATDCs. CD133-positive cells generated SA$^-$ (red)/GATA-4$^+$ (green) cells (a), cardiac troponin T$^+$ (red)/GATA-4$^+$ (green) cells (c), or cardiac troponin I$^-$ (red)/MEF2C$^+$ (green) cells (e). Nuclear staining by TOPRO3 in a, c, and e is shown in b, d, and f, respectively. Notably, well-organized sarcomeres, Z-band, and a large number of mitochondria were observed in CD133$^+$ BATDCs. Scale bar = 10 μm (f) and 1 μm (g). **(C):** a, Existence of SA-positive (green) and GATA4-positive (red) CMs in the culture of CD133+ BATDCs. b, Nuclear staining with 4,6-diamidino-2-phenylindole in the same field as shown in panel a. Note that this low-power field view clearly showed that approximately 50% of adherent cells are CMs. Scale bar = 20 μm. c, Quantitative evaluation of differentiation potential for CMs from each fraction of BATDCs as indicated. The same number of cells (1×10^4) of each fraction was cultured. Note that c-Kit$^+$ (CD45$^-$ter119$^-$CD31$^-$) cells could not differentiate into CMs, and CD133$^+$ (CD45$^-$ter119$^-$CD31$^-$) cells were the most effective at differentiating into CMs.

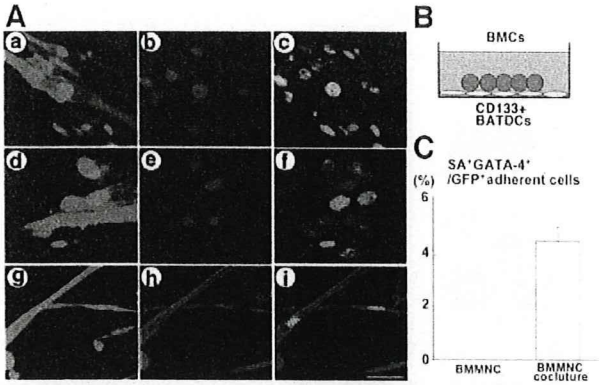

Figure 2. BMMNCs can differentiate into cardiomyocytes (CMs) upon coculturing with BATDCs. **(A):** Immunocytochemical analysis of BMMNCs from green mice cocultured for 14 days with CD133-positive BATDCs from wild-type mice. a–c, GFP (green) (a), GATA-4 (red) (b), and nuclear staining with TOPRO3 (blue) merged with that shown in b (c). d–f, GFP (green) (d), MEF2C (red) (e), and nuclear staining with TOPRO3 (blue) merged with that shown in e (f). g–I, GFP (green) (g), SA (red) (h), and GATA-4 (blue) merged with that shown in h (i). Scale bar = 5 μm (i). **(B):** Schematic presentation of coculturing BMMNCs from green mice with CD133-positive BATDCs from wild-type mice. **(C):** Quantitative evaluation of differentiated SA- and GATA4-positive CMs among adhering GFP-positive BM-derived cells. Data for BMMNC cocultured with CD133+ BATDCs and BMMNCs cultured alone are displayed. Results represent the mean of five independent experiments. Abbreviations: BATDC, brown adipose tissue-derived cell; BMC, bone marrow cell; BMMNC, bone marrow mononuclear cell; GFP, green fluorescent protein.

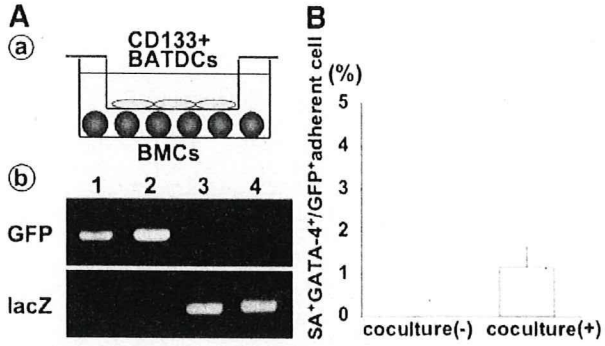

Figure 3. Bone marrow mononuclear cells (BMMNCs) differentiated into cardiomyocytes (CMs) in separated coculture system. **(A):** a, Schematic representation of the system for the separate coculture of BMMNCs with $CD133^+$ BATDCs. b, Reverse transcription-polymerase chain reaction analysis in separate culture conditions. BMMNCs were derived from green mice (lower chamber), and BATDCs were derived from ROSA26 mice (upper chamber). GFP signal was detected only in the lower chamber, and lacZ signal was detected only in the upper chamber. Lane 1, BMMNCs before culture (lower chamber); lane 2, BMMNCs after 14 days of culture (lower chamber); lane 3, BATDCs before culture; lane 4, BATDCs after 14 days of culture. **(B):** Quantitative evaluation of the differentiation potential for CMs from BMMNCs in separate culture conditions. Upon coculturing with BATDCs (coculture[+]), approximately 1.7% of adhering GFP-positive bone marrow cells differentiated into SA- and GATA4-positive CMs. CM development could not be observed when BMMNCs were cultured alone (coculture[−]). Results represent the mean of five independent experiments. Abbreviations: BATDC, brown adipose tissue-derived cell; BMC, bone marrow cell; GFP, green fluorescent protein.

BATDCs Effectively Induce CM Production from BMCs

A previous in vitro study showed that although BMCs were a source of CMs, they could not spontaneously differentiate into CMs; however, differentiation could be induced with 5-azacytidine, a DNA-hypomethylating agent [4]. It is thought that BMCs can differentiate into CMs upon adequate environmental molecular cues. As $CD133^+$ BATDCs differentiate into CMs spontaneously, this suggests that $CD133^+$ BATDCs produce molecules that induce the differentiation of $CD133^+$ BATDCs into CMs by an autocrine loop. Therefore, to test this ability, we cultured BMMNCs with BATDCs and observed whether or not, under these conditions, BMMNCs could differentiate into CMs. At first, $CD133^+$ cells were sorted from BAT by FACS and cultured on 0.1% gelatin-coated dishes. After 1 week, BMMNCs derived from green mice that express GFP ubiquitously in their tissues [28] were cocultured in direct contact with $CD133^+$ BATDCs, as shown in Figure 2B. By coculturing BMMNCs with CD133-positive BATDCs, nuclear-located GATA-4-positive (Fig. 2A, a–c), MEF2C-positive (Fig. 2A, d–f), and SA-positive (Fig. 2A, g–i) contracting cells were produced among the GFP-positive BMMNCs. However, the SA-positive and GATA-4-positive cells were not observed when BMMNCs were cultured alone under the same conditions (Fig. 2C).

BMMNCs with BATDCs Differentiated into CMs Without Fusion Mechanism

Recently, it has been suggested that cell fusion is the main mechanism that contributes to the development or maintenance of cardiac muscle and neuron regeneration [8, 29]. To exclude the possibility of cell fusion in our experiment, we cultured BMMNCs from green mice with BATDCs from ROSA26 mice, which express LacZ ubiquitously in their tissues, and separated the cells from these two different origins with a 0.4-μm-pore membrane (Fig. 3A, a). In this separating coculture system, $SA^+GATA\text{-}4^+$ CMs were also produced from BMMNCs when cocultured with BATDCs (Fig. 3B). Moreover, with PCR analysis, GFP-positive signals were detected only in the BMMNC layer, and lacZ-positive signals were detected only in the BATDCs layer from the cells before and after culturing (Fig. 3A, b). Therefore, we concluded that the development of CMs from BMMNCs was not dependent on cell fusion with BATDCs.

Cell Contact Mediated by Bivalent Cation Is Critical for the Differentiation of BMMNCs into CMs

We found that BMMNCs could differentiate into CMs under conditions in which the BMMNCs were cultured in direct or indirect contact with BATDCs; however, differentiation of BMMNCs into CMs was promoted more effectively by direct cell-to-cell contact between BMMNCs and BATDCs than under separated culture conditions (Figs. 2B, 3B). Indeed, 520 ± 40 versus 105 ± 18 SA^+GATA4^+ CMs were generated from 1×10^5 BMMNCs under direct and indirect cocultures, respectively. To exclude the possibility of cell fusion in the contact coculture system, we used paraformaldehyde-fixed cultured $CD133^+$ BATDCs, which cannot fuse with other cells but have an intact cell surface. After coculturing with fixed BATDCs, some GFP^+ BMMNC-derived cells (Fig. 4A, a) expressed cardiac-specific antigens, such as SA (Fig. 4A, b and c), GATA-4, and cardiac troponinT (data not shown). Moreover, these cells also had the typical features of CMs, confirmed by electron microscopic analysis (Fig. 4A, f).

Cadherin-mediated calcium-dependent cell-to-cell contact is widely believed to be involved in the regulation of the diverse signaling process for cell differentiation [30]. Therefore, we elucidated a potential role for calcium-dependent cell-to-cell contact in our coculture system. First, BMMNCs were incubated with the calcium chelator EDTA or EGTA on fixed BATDCs. This treatment abolished the adhesion of BMMNCs to fixed, differentiated BATDCs. By the suppression of cell adhesion of BMCs to differ-